Hepatology Research 2008; 38: 310–314 doi: 10.1111/j.1872-034X.2007.00263.x

Short Communication

Prevalence of hepatitis B virus infection in Japanese patients with HIV

Kazuhiko Koike,[1] Yoshimi Kikuchi,[2] Michio Kato,[3] Junki Takamatsu,[4] Yoshizumi Shintani,[1] Takeya Tsutsumi,[1] Hajime Fujie,[1] Hideyuki Miyoshi,[1] Kyoji Moriya[1] and Hiroshi Yotsuyanagi[1]

[1]Department of Internal Medicine, Graduate School of Medicine, University of Tokyo, Tokyo, [2]AIDS Clinical Center, International Medical Center of Japan, Tokyo, [3]Department of Gastroenterology, Osaka National Hospital, Osaka and [4]Department of Transfusion Medicine, Nagoya University Hospital, Nagoya, Japan

Patients with HIV infection are frequently infected with hepatitis viruses, which are presently the major cause of mortality in HIV-infected patients after the widespread use of highly active antiretrovirus therapy. We previously reported that approximately 20% of HIV-positive Japanese patients were also infected with hepatitis C virus (HCV). Hepatitis B virus (HBV) infection may also be an impediment to a good course of treatment for HIV-infected patients, because of recurrent liver injuries and a common effectiveness of some anti-HIV drugs on HBV replication. However, the status of co-infection with HIV and HBV in Japan is unclear. We conducted a nationwide survey to determine the prevalence of HIV–HBV co-infection by distributing a questionnaire to the hospitals belonging to the HIV/AIDS Network of Japan. Among the 5998 patients reported to be HIV positive, 377 (6.4%) were positive for the hepatitis B surface antigen. Homosexual men accounted for two-thirds (70.8%) of the HIV–HBV co-infected patients, distinct from HIV–HCV co-infection in Japan in which most of the HIV–HCV co-infected patients were recipients of blood products. One-third of HIV–HBV co-infected patients had elevated serum alanine aminotransferase levels at least once during the 1-year observation period. In conclusion, some HIV-infected Japanese patients also have HBV infection and liver disease. A detailed analysis of the progression and activity of liver disease in co-infected patients is needed.

Key words: co-infection, hepatitis B, HIV, liver disease.

INTRODUCTION

HEPATITIS B VIRUS (HBV) infection is a major public health problem worldwide, along with hepatitis C virus (HCV) and HIV infections. In the USA, the estimated prevalence of HBV is less than 1%, but approximately 1 million people are persistently infected.[1] The prevalence of HIV in the USA is also <1%, and the virus is estimated to have infected approximately 800 000 people.[2] Because of the common transmission routes, that is, parenteral transmission routes, many people with HIV infection are also infected with HBV. Among the HIV-positive people in the USA, the prevalence of HBV co-infection is 6–14%.[1,2] Before the introduction of highly active antiretroviral therapy (HAART) in 1996, most patients with HIV infection died of HIV-associated opportunistic infections, such as *Pneumocystis jiroveci* pneumonia and cytomegaloviral infection. Since the widespread use of HAART, the mortality associated with HIV infection has declined. However, the reduction in mortality due to opportunistic infection, has left patients co-infected with HIV and hepatitis viruses faced with the menace of progressive liver diseases due to HBV infection,[3,4] in addition to HCV infection.[5]

HBV co-infection or superinfection of HIV-infected patients leads to several problematic situations. First, HBV infection tends to develop into persistent infection in HIV-infected patients,[1,6,7] which is a rare event in healthy adults, although it substantially depends on the genotype of HBV.[8] It results in the acceleration of the development of cirrhosis and eventually hepatocellular carcinoma. Second, some nucleoside reverse transcriptase inhibitors (NRTI) used in HAART also have

Correspondence: Professor Kazuhiko Koike, Department of Infectious Diseases, Internal Medicine, Graduate School of Medicine, University of Tokyo, 7-3-1 Hongo, Bunkyo-ku, Tokyo 113-8655, Japan. Email: kkoike-tky@umin.ac.jp

Received 22 June 2007; revision 29 July 2007; accepted 31 July 2007.

inhibitory effects on the replication of HBV.[9–12] A careless administration or discontinuation of NRTI on HIV–HBV co-infected patients may cause reactivation and/or aggravation of hepatitis B. In addition, the administration of anti-HBV drugs in HIV–HBV co-infection may lead to the development of drug resistance.[11,12] Third, liver injury occurs more frequently in patients on HAART who are co-infected with HIV and HBV than those infected with HIV only.[9,10]

Importantly, co-infection with HIV and HCV increases the morbidity and mortality of HIV-infected patients in Japan,[13] where the prevalence of HIV infection is increasing linearly, and is exceptionally high among developed countries.[14] There are more than 14 000 HIV-positive people in Japan as of 2006, according to the AIDS National Survey in Japan,[14] and approximately 0.8 million chronic HBV carriers.[15] However, the prevalence of co-infection with HIV and HBV in Japan has not been clarified to date. Therefore, we conducted a nationwide study by distributing a postal mail-based questionnaire to the hospitals belonging to the HIV/AIDS Network of Japan.

PATIENTS AND METHODS

IN THE QUESTIONNAIRE, the following information was obtained from the hospitals regarding the number of patients who visited the hospitals at least once between January and December in 2006: (i) the number of HIV-positive patients; (ii) the number of hepatitis B surface antigen (HBsAg)-positive patients among (i); (iii) the number of patients among (ii) who were determined at least once to have a serum alanine aminotransferase (ALT) level higher than 100 IU/L; (iv) the number of HIV-positive patients that contracted HIV from blood products; (v) the number of HBsAg-positive patients among (iv), (vi) the number of patients among (v) who were determined at least once to have a serum ALT level higher than 100 IU/L; (vii) the number of HIV-positive patients among homosexual men, (viii) the number of HBsAg-positive patients among (vii), (ix) the number of patients among (viii) who were determined at least once to have a serum ALT level higher than 100 IU/L; (x) the number of HIV-positive patients that contracted HIV through intravenous drug use (xi) the number of HBsAg-positive patients among (x), (xii) the number of patients among (xi) who had at least one determination of a serum ALT level more than 100 IU/L; (xiii) the number of HIV-positive patients whose transmission routes were classified as "others"; (xiv) the number of HBsAg-positive patients among (xiii); and (xv) the number of patients among (xiv) who were determined at least once to have a serum ALT level higher than 100 IU/L.

The questionnaire was sent to the 372 hospitals belonging to the HIV/AIDS Network of Japan by mail. Answers were mostly returned by mail and in some cases by fax. The list of the hospitals in the HIV/AIDS Network of Japan can be viewed at http://www.acc.go.jp/mLhw/mLhw_frame.htm.

RESULTS

THE QUESTIONNAIRE WAS sent to all 372 hospitals that were on the list of the hospitals in the HIV/AIDS Network of Japan in January 2006. Two hundred and seven hospitals (55.6%) responded within the indicated period. In total, 5998 patients were reported to be HIV positive. The collection rate of 55.6% was higher than that (47.8%) for a questionnaire HIV–HCV co-infection study carried out in 2003.[15] It may appear rather low, particularly considering the number of reported HIV-positive people in 2006, which was approximately 14 000, according to the AIDS National Survey in Japan.[14] However, not all of the HIV-positive people were going to hospitals, and the answers to the questionnaire were obtained from most of the major hospitals in the HIV/AIDS Network in big cities around Japan. This suggests that not all, but a majority of HIV-positive Japanese patients were enrolled in the study.

Among the 5998 patients reported to be HIV positive, 377 (6.3%) patients were positive for HBsAg (Table 1). Of these 377 patients, 122 (32.4%) had elevated serum ALT levels at least one time during the 1-year observation period.

The HBV prevalence rates, when fractionated by the routes of transmission, were as follows: among the 508 HIV-positive patients who contracted HIV from blood products, such as unheated concentrated coagulation factors, only 30 (5.9%) were HBsAg positive, which shows a marked contrast to the prevalence of HCV in this cohort (Fig. 1).[16] Among the 23 intravenous drug users, three (13.0%) were HBsAg positive. Among the 3213 HIV-positive patients who were homosexual men, 267 (8.3%) were HBsAg positive. In the remaining 2254 patients who were HIV-positive and whose route of HIV transmission was classified as "others", most contracted HIV heterosexually. This number (2254) showed a substantial increase from the 1316 obtained in the questionnaire for the HIV–HCV co-infection study in 2003, while the total number of HIV-positive patients increased from 4877 to 5998.[16] Among these, 77 (3.4%)

Table 1 Prevalence rates of hepatitis B virus infection among HIV-positive patients

Routes of transmission	No. patients	HBsAg positive (% in HIV positive according to route)	ALT >100 IU/L (% in HBsAg positive according to route)
Blood products	508 (5.9%)	30 (40.0%)	12
Homosexual men	3213 (8.3%)	267 (32.2%)	86
Drug addicts	23 (13.0%)	3 (66.7%)	2
Others (heterosexual etc.)	2254 (3.4%)	77 (28.6%)	22
Total	5998	377 (6.3%)	122 (32.4%)

ALT, serum alanine aminotransferase; HBsAg, hepatitis B surface antigen.

were HBsAg positive. In terms of the route of HIV infection, 267 (70.8%) of the 377 patients were homosexual men among the HIV–HBV co-infected patients. This shows a contrast to the status of HIV–HCV co-infection, in which the majority of HIV–HCV co-infected Japanese patients contracted both viruses from blood products.[16]

There were one or more HIV-positive patients in 154 (74.4%) of the 207 hospitals in the HIV/AIDS Network of Japan (Table 2). Twenty four (11.6%) of 207 hospitals had 20–49 HIV-positive patients, and 16 (7.7%) hospitals had 50 or more HIV-positive patients. There were one or more patients who were co-infected with HIV and HBV in 64 (30.9%) of the 207 hospitals. There were 10 or more HIV–HBV co-infected patients in nine (4.3%) hospitals, all of which had 50 or more HIV-positive patients (Table 2). HIV–HBV co-infected patients were concentrated in specific hospitals in big cities around Japan. In particular, in the Kanto area, HIV–HBV co-infected patients were concentrated in the HIV/AIDS Network hospitals in the Tokyo city area.

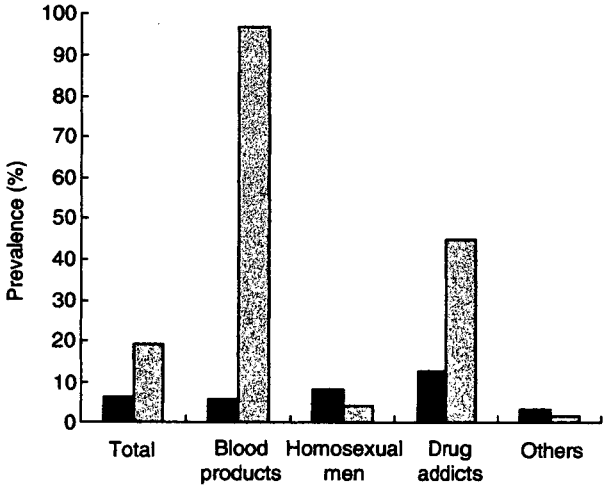

Figure 1 Prevalence rates of persistent hepatitis B virus and hepatitis C virus infections in the HIV-positive population sorted by the HIV risk group. (■), HBsAg, hepatitis B surface antigen; (▨), anti-HCV, antibody to hepatitis C virus. *Prevalence rates of anti-HCV are obtained from Koike K *et al.*[16]

DISCUSSION

ALONG WITH THE increase in the number of HIV-infected patients in Japan, co-infection with HIV and hepatitis viruses has become a major medical issue. HBV infection of HIV-positive patients raises several difficult problems: HBV infection tends to develop into persistent infection, even in adults; some NRTI used in HAART also have inhibitory effects on the replication of HBV, the improper administration, or discontinuation of which may lead to drug resistance; and HIV–HBV co-infected patients on HAART have liver injuries more frequently than HIV-monoinfected patients. It is important to determine the status of HBV infection in HIV-positive patients.

According to the statistics of the Ministry of Health, Labor, and Welfare of Japan, the number of reported HIV-positive people was slightly over 14 000 in 2006.[14] In the present study, 6.4% of HIV-positive patients were positive for HBsAg, the most reliable marker for ongoing HBV infection. It might have been advantageous if

Table 2 Number of hospitals categorized according to the number of patients infected with HIV and those co-infected with HIV and hepatitis B virus (HBV)

No. HIV (+)/ HBV (+)	No. HIV(+)				
	0	1–19	20–49	50+	Total
0	53	76	13	1	143
1–9	0	38	11	6	55
10+	0	0	0	9	9
Total	53	114	24	16	207

serum HBV-DNA levels were determined, but unfortunately, HBV-DNA level determination was not a routine laboratory test in most hospitals. In addition, considering that the antibody to the hepatitis B core antigen might be the only marker of ongoing HBV infection in some immuno-compromised patients, it would also be advantageous if this viral marker were available. These issues should be investigated in future studies. Comments from hospitals to the questionnaire included one indicating that not all HIV-positive patients underwent a test for serum HBsAg, suggesting the actual prevalence of HBsAg in HIV-infected patients might be higher than 6.4%.

In a previous questionnaire study of HIV–HCV co-infection, the prevalence of HCV infection among HIV-infected patients was 19.2%;[16] the prevalence of HBV infection (6.4%), is one-third of it. The lower positivity for HBsAg than for the anti-HCV antibody among those who contracted HIV through blood products accounts for this difference: almost all (96.9%) of the patients who contracted HIV through blood products were also anti-HCV antibody positive.[16] It should be noted that among the homosexual male patients who were HIV positive, 8.3% were HBsAg positive, which is twice as high as that of the anti-HCV antibody in these populations. A higher prevalence of HBV infection as a sexually transmitted infection than that of HCV[17] may explain the high prevalence of HBV infection in HIV-positive homosexual men. Similarly, a HBV prevalence of 3.4% in heterosexually transmitted HIV-positive patients is higher than that of the general Japanese population of the same age.[15]

Of the 377 patients who were HBsAg positive, 122 (32.4%) had elevated serum ALT levels at least once in the 1-year observation period. In this type of study using a questionnaire, it is difficult to obtain the details of patients' data, including age, body weight, and the degrees of liver injuries and fibrosis. If detailed items were included in the questionnaire, then the collection rate would be low. This time, to obtain a high collection rate, we asked whether the patients with HBsAg showed an elevated ALT level higher than 100 IU/L at least once during the 1-year observation period. We thereby do not have details on liver disease in HIV–HBV co-infected patients in the current study. Nonetheless, one-third of HIV–HBV co-infected patients have moderate liver injuries, either chronic hepatitis B or adverse effects of drugs, and are waiting for an aid for the amelioration of liver disease. A detailed analysis of the progression and activity of liver disease in HIV–HBV co-infected patients is expected.

The collection rate of the present questionnaire from the hospitals belonging to the HIV/AIDS Network was 55.6% (207 of 372). This was higher than that (47.8%) in the HIV–HCV co-infection questionnaire study carried out in 2003. The reason for this increase is not clear, but presumably the questionnaire conducted in 2003 has raised awareness among hospital staff regarding the relevance of hepatitis virus and HIV co-infection in clinical practice.

In the current study, both Japanese patients and those of other nationalities/ethnicities were included in the study. Although the ratio of newly diagnosed HIV-positive foreign people has been declining to approximately 10% in 2006, the one in total HIV positive still accounts for approximately 25% in Japan. Because the rates of the HBV carrier are different among countries, it is ideal to analyze the HBV prevalence separately according to the nationalities/ethnicities. However, in the current survey to the hospitals in HIV/AIDS Network of Japan, nationality/ethnicity was not itemized in order to make the questionnaire simple. If we would attempt to obtain such data under the approval of the ethical committee in each hospital, the response rate to questionnaire would be extremely lowered.

To establish measures that decrease the morbidity and mortality of HIV–HBV co-infected patients, it is essential to determine the current status of co-infection. In the present study, the number and transmission routes of HIV–HBV co-infected patients in Japan were determined for the first time, although detailed information on the severity and progression of liver disease in HIV–HBV co-infected patients has not been obtained yet. Undoubtedly, this will be the first step towards improving the prognosis and quality of life of Japanese patients co-infected with HIV and HBV.

ACKNOWLEDGMENTS

WE THANK MS. Ogawa for her assistance in the questionnaire inquiry. This work was supported in part by Health Sciences Research Grants from the Ministry of Health, Labor, and Welfare of Japan (Research on HIV/AIDS). We thank the hospitals in the HIV/AIDS Network of Japan for the responses to the questionnaire. The list of hospitals can be view at http://www.acc.go.jp/mLhw/mLhw_frame.htm.

REFERENCES

1 Alter MJ. Epidemiology of viral hepatitis and HIV coinfection. *J Hepatol* 2006; 44: S6–9.

2 Sherman KE, Peters M, Koziel MJ. HIV and liver disease forum: conference proceedings. *Hepatology* 2007; **45**: 1566–77.
3 Hoffmann CJ, Thio CL. Clinical implications of HIV and hepatitis B co-infection in Asia and Africa. *Lancet Infect Dis* 2007; **7**: 402–9.
4 Maida I, Soriano V, Castellares C *et al.* Liver fibrosis in HIV-infected patients with chronic hepatitis B extensively exposed to antiretroviral therapy with anti-HBV activity. *HIV Clin Trials* 2006; **7**: 246–50.
5 Bica I, McGovern B, Dhar R *et al.* Increasing mortality due to end-stage liver disease in patients with human immunodeficiency virus infection. *Clin Infect Dis* 2001; **32**: 492–7.
6 Weinbaum CM, Sabin KM, Santibanez SS. Hepatitis B, hepatitis C, and HIV in correctional populations: a review of epidemiology and prevention. *AIDS* 2005; **19**: S41–6.
7 Salmon-Ceron D, Lewden C, Morlat P *et al.* Liver disease as a major cause of death among HIV infected patients: role of hepatitis C and B viruses and alcohol. *J Hepatol* 2005; **42**: 799–805.
8 Ozasa A, Tanaka Y, Orito E *et al.* Influence of genotypes and precore mutations on fulminant or chronic outcome of acute hepatitis B virus infection. *Hepatology* 2006; **44**: 326–34.
9 Thio CL, Locarnini S. Treatment of HIV/HBV coinfection: clinical and virologic issues. *AIDS Rev* 2007; **9**: 40–53.
10 Sulkowski MS. Hepatotoxicity associated with antiretroviral therapy containing HIV-1 protease inhibitors. *Semin Liver Dis* 2003; **23**: 183–94.
11 Jain MK, Comanor L, White C *et al.* Treatment of hepatitis B with lamivudine and tenofovir in HIV/HBV-coinfected patients: factors associated with response. *J Viral Hepat* 2007; **14**: 176–82.
12 Quarleri J, Moretti F, Bouzas MB *et al.* Hepatitis B virus genotype distribution and its lamivudine-resistant mutants in HIV-coinfected patients with chronic and occult hepatitis B. *AIDS Res Hum Retroviruses* 2007; **23**: 525–31.
13 Tatsunami S, Taki M, Shirahata A, Mimaya J, Yamada K. Increasing incidence of critical liver disease among causes of death in Japanese hemophiliacs with HIV-1. *Acta Haematol* 2004; **111**: 181–4.
14 The Ministry of Health, Labor and Welfare of Japan. *National AIDS Survey Report*, 2004. [Cited 2007.] Available from URL: http://www.wam.go.jp/wamappl/bb14GS50.nsf/vAdmPBigcategory40/727FDBF7F51718B5492572C800071D25?Open Document
15 Tanaka J, Kumagai J, Katayama K *et al.* Sex- and age-specific carriers of hepatitis B and C viruses in Japan estimated by the prevalence in the 3 485 648 first-time blood donors during 1995–2000. *Intervirology* 2004; **47**: 32–40.
16 Koike K, Tsukada K, Yotsuyanagi H *et al.* Prevalence of coinfection with human immunodeficiency virus and hepatitis C virus in Japan. *Hepatol Res* 2007; **37**: 2–5.
17 Denis F, Adjide CC, Rogez S, Delpeyroux C, Rogez JP, Weinbreck P. Seroprevalence of HBV, HCV and HDV hepatitis markers in 500 patients infected with the human immunodeficiency virus. *Pathol Biol (Paris)* 1997; **45**: 701–8.

Research article

PPARα activation is essential for HCV core protein–induced hepatic steatosis and hepatocellular carcinoma in mice

Naoki Tanaka,[1,2] Kyoji Moriya,[3] Kendo Kiyosawa,[2] Kazuhiko Koike,[3] Frank J. Gonzalez,[4] and Toshifumi Aoyama[1]

[1]Department of Metabolic Regulation, Institute on Aging and Adaptation, Shinshu University Graduate School of Medicine, Matsumoto, Nagano, Japan.
[2]Division of Gastroenterology, Department of Internal Medicine, Shinshu University School of Medicine, Matsumoto, Nagano, Japan.
[3]Department of Infectious Diseases, Internal Medicine, Graduate School of Medicine, University of Tokyo, Tokyo, Japan.
[4]Laboratory of Metabolism, National Cancer Institute, NIH, Bethesda, Maryland, USA.

Transgenic mice expressing HCV core protein develop hepatic steatosis and hepatocellular carcinoma (HCC), but the mechanism underlying this process remains unclear. Because PPARα is a central regulator of triglyceride homeostasis and mediates hepatocarcinogenesis in rodents, we determined whether PPARα contributes to HCV core protein–induced diseases. We generated PPARα-homozygous, -heterozygous, and -null mice with liver-specific transgenic expression of the core protein gene (*Ppara*$^{+/+}$:HCVcpTg, *Ppara*$^{+/-}$:HCVcpTg, and *Ppara*$^{-/-}$:HCVcpTg mice. Severe steatosis was unexpectedly observed only in *Ppara*$^{+/+}$:HCVcpTg mice, which resulted from enhanced fatty acid uptake and decreased mitochondrial β-oxidation due to breakdown of mitochondrial outer membranes. Interestingly, HCC developed in approximately 35% of 24-month-old *Ppara*$^{+/+}$:HCVcpTg mice, but tumors were not observed in the other genotypes. These phenomena were found to be closely associated with sustained PPARα activation. In *Ppara*$^{+/-}$:HCVcpTg mice, PPARα activation and the related changes did not occur despite the presence of a functional *Ppara* allele. However, long-term treatment of these mice with clofibrate, a PPARα activator, induced HCC with mitochondrial abnormalities and hepatic steatosis. Thus, our results indicate that persistent activation of PPARα is essential for the pathogenesis of hepatic steatosis and HCC induced by HCV infection.

Introduction

HCV is one of the major causes of chronic hepatitis, whereas patients with persistent HCV infection have a high incidence of hepatocellular carcinoma (HCC) (1, 2). Occurrence of HCC associated with chronic HCV infection has increased over the past 2 decades (3–5), and chronic HCV infection is recognized as a serious debilitating disease. However, the mechanism in which chronic HCV infection mediates hepatocarcinogenesis remains unclear.

HCV core protein was shown to have oncogenic potential (6). To examine how HCV core protein participates in HCV-related hepatocarcinogenesis, transgenic mouse lines were established in which HCV core protein is expressed constitutively in liver at cellular levels similar to those found in chronic HCV-infected patients (7). These mice exhibited hepatic steatosis (7) and insulin resistance (8) as early as 3 months of age; on further aging, these symptoms worsened and hepatic adenomas developed in approximately 30% of mice between 16 and 18 months of age (9). Finally, HCC was found within hepatic adenomas in a classic "nodule-in-nodule" pathology (9). Interestingly, no hepatic inflammation or fibrosis was found in these mice throughout the course of HCC development (9), which suggested that the HCV core protein itself induces hepatic steatosis and HCC independently of hepatitis.

Several studies support the contention that hepatic steatosis promotes the development of HCC (10). Epidemiologic data have identified hepatic steatosis as a major accelerating factor of hepatocarcinogenesis in chronic HCV-infected patients (11). Moreover, increases in ROS production that can cause oxidative DNA damage, mitochondrial abnormalities, and accelerated hepatocyte proliferation were observed in the steatotic livers (12–14). Thus, an intriguing possibility has emerged that alteration of fatty acid metabolism in hepatocytes may be central to the pathogenesis of HCC induced by HCV core protein.

PPARs are ligand-activated nuclear receptors belonging to the steroid/thyroid hormone receptor superfamily; 3 isoforms designated as α, β/δ, and γ exist, all of which are involved in lipid homeostasis (15). PPARα regulates constitutive transcription of genes encoding fatty acid–metabolizing enzymes (16) and is associated with the maintenance of fatty acid transport and metabolism, primarily in liver, kidney, and heart. Administration of PPARα agonists, such as the widely prescribed fibrate drugs clofibrate, gemfibrozil, and fenofibrate, ameliorate hyperlipidemia in humans (17) and hepatic steatosis in mice (18).

On the other hand, long-term administration of PPARα ligands to rodents causes accelerated hepatocyte proliferation, increased ROS generation, and development of HCC (19, 20). Disruption of the PPARα gene was shown to prevent the development of HCC caused by long-term exposure to PPARα activators (21). Interestingly, accumulation of fatty acids/triglycerides in hepatocytes

Nonstandard abbreviations used: ACC, acetyl-CoA carboxylase; AOX, acyl-CoA oxidase; CDK, cyclin-dependent kinase; CYP4A1, cytochrome P450 4A1; FAS, fatty acid synthase; FAT, fatty acid translocase; FATP, fatty acid transport protein; HCC, hepatocellular carcinoma; HCVcpTg, HCV core protein–expressing transgenic; L-FABP, liver fatty acid-binding protein; MCAD, medium-chain acyl-CoA dehydrogenase; MTP, microsomal transfer protein; 8-OHdG, 8-hydroxy-2′-deoxyguanosine; PCNA, proliferating cell nuclear antigen; RXRα, retinoid X receptor α.

Conflict of interest: The authors have declared that no conflict of interest exists.

Citation for this article: *J. Clin. Invest.* 118:683–694 (2008). doi:10.1172/JCI33594.

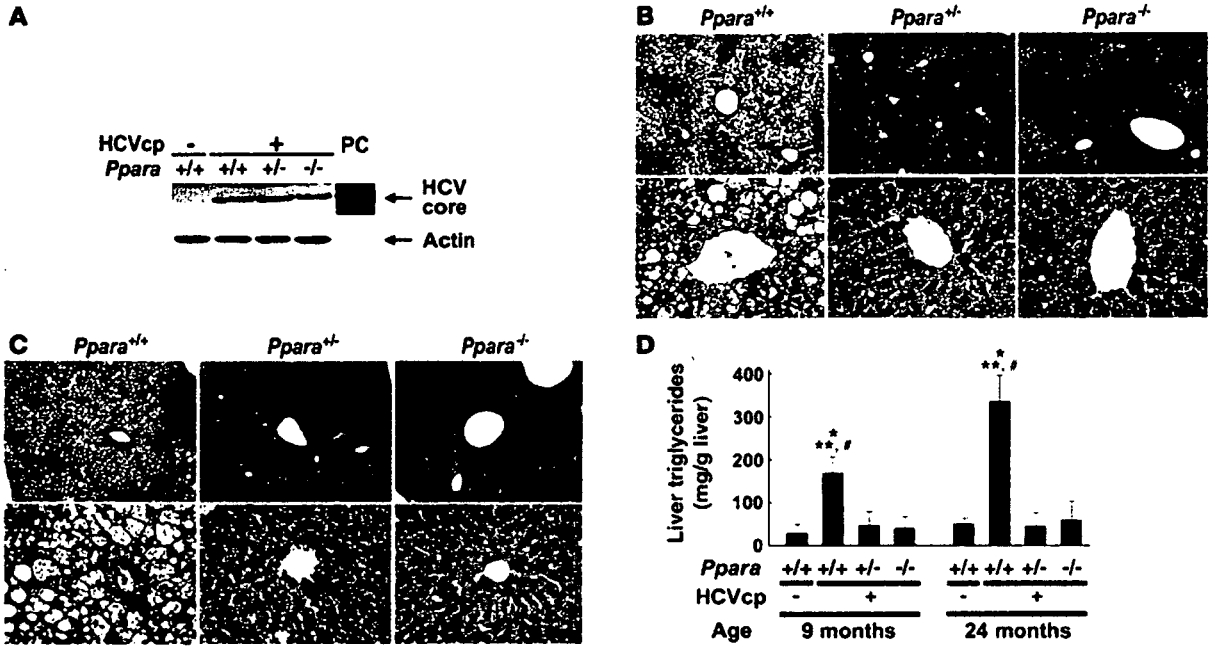

Figure 1

Phenotype changes in transgenic mouse liver. (**A**) Immunoblot analysis of HCV core protein expression in livers of 9-month-old mice. Because no significant individual differences in the same mouse group were found in the preliminary experiments, 10 mg of liver prepared from each mouse ($n = 6$ /group) was mixed and homogenized. Whole-liver lysate (50 μg protein) was loaded in each well. The band of actin was used as the loading control. Results are representative of 4 independent experiments. PC, lysate prepared from COS-1 cells overexpressing HCV core protein as a positive control. (**B**) Histological appearance of hematoxylin- and eosin-stained liver sections from 9-month-old HCVcpTg mice. Upper and lower rows show a lower (×40) and higher (×400) magnification, respectively. Microvesicular and macrovesicular steatosis was found only in *Ppara*$^{+/+}$:HCVcpTg mice. No inflammation or hepatocyte degeneration was evident in any of the genotypes. (**C**) Histological appearance of hematoxylin- and eosin-stained liver sections from 24-month-old HCVcpTg mice. Upper and lower rows show a lower (×40) and higher (×400) magnification, respectively. Hepatic steatosis was marked in *Ppara*$^{+/+}$:HCVcpTg mice, but not in other mice. Hepatic inflammation, fibrosis, and hepatocyte degeneration were not observed. In *Ppara*$^{+/-}$:HCVcpTg and *Ppara*$^{-/-}$:HCVcpTg mice, dysplastic hepatocytes and precancerous lesions were not detected throughout the entire liver. (**D**) Content of liver triglycerides. Results are expressed as the mean ± SD ($n = 6$/group) and compared between genotypes at the same age. $^{*}P < 0.05$ compared with *Ppara*$^{+/+}$ nontransgenic mice; $^{**}P < 0.05$ compared with *Ppara*$^{+/-}$:HCVcpTg mice; $^{\#}P < 0.05$ compared with *Ppara*$^{-/-}$:HCVcpTg mice.

could lead to continuous PPARα activation because of the presence of fatty acid metabolites that serve as natural PPARα ligands. For example, mice lacking expression of the peroxisomal acyl-CoA oxidase (AOX) gene showed massive accumulation of very-long-chain fatty acids in hepatocytes, severe microvesicular steatosis, chronic PPARα activation, and development of hepatic adenoma and HCC by 15 months of age (22). These results suggest a strong contribution of activated PPARα to liver tumorigenesis.

On the basis of several lines of evidence, we hypothesized that PPARα might contribute to hepatocarcinogenesis in HCV core protein-expressing transgenic (HCVcpTg) mice. To explore this possibility, PPARα-homozygous (*Ppara*$^{+/+}$), PPARα-heterozygous (*Ppara*$^{+/-}$), and PPARα-null (*Ppara*$^{-/-}$) mice bearing the HCV core protein gene, designated *Ppara*$^{+/+}$:HCVcpTg, *Ppara*$^{+/-}$:HCVcpTg, and *Ppara*$^{-/-}$:HCVcpTg mice, were generated, and phenotypic changes were examined. Surprisingly, we found that severe hepatic steatosis and HCC induced by HCV core protein developed only in *Ppara*$^{+/+}$ mice, which were related to persistent PPARα activation.

Results

Expression of HCV core protein in transgenic mice. *Ppara*$^{-/-}$:HCVcpTg and *Ppara*$^{+/-}$:HCVcpTg mice appeared healthy, and body weight in both genotypes was similar to that of *Ppara*$^{+/+}$:HCVcpTg and *Ppara*$^{+/+}$ mice without the transgene. When hepatic expression of HCV core protein in 9-month-old transgenic mice was examined by immunoblot analysis, it was similar among *Ppara*$^{+/+}$:HCVcpTg, *Ppara*$^{+/-}$:HCVcpTg, and *Ppara*$^{-/-}$:HCVcpTg mice (Figure 1A) and was also similar to expression in HCVcpTg mice reported previously (7, 9). Age and sex had only a minor influence on the hepatic expression of HCV core protein.

Requirement of homozygous PPARα for the development of hepatic steatosis in transgenic mice. Livers of 9-month-old male HCVcpTg mice with or without the *Ppara* allele were examined. Those of *Ppara*$^{+/+}$:HCVcpTg mice were soft, slightly enlarged, and light in color and histologically showed macrovesicular and microvesicular steatosis with no apparent inflammation or hepatocyte necrosis (Figure 1B), in agreement with previous reports (7, 9). Biochemical analysis of liver extracts showed marked hepatic accumulation of triglycerides (Figure 1D). In contrast, livers of 9-month-old *Ppara*$^{+/-}$:HCVcpTg and *Ppara*$^{-/-}$:HCVcpTg mice showed neither histological abnormalities nor accumulation of triglycerides (Figure 1, B and D). Hepatic levels of free fatty acids in *Ppara*$^{+/+}$:HCVcpTg mice were approximately 3 times those in *Ppara*$^{+/-}$:HCVcpTg and *Ppara*$^{-/-}$:HCVcpTg mice or *Ppara*$^{+/+}$ mice not expressing the HCV core protein.

In 24-month-old *Ppara*$^{+/+}$:HCVcpTg mice, hepatic steatosis was found (Figure 1C), and the hepatic levels of triglycerides were further increased (Figure 1D). Apparent inflammation, hepatocyte

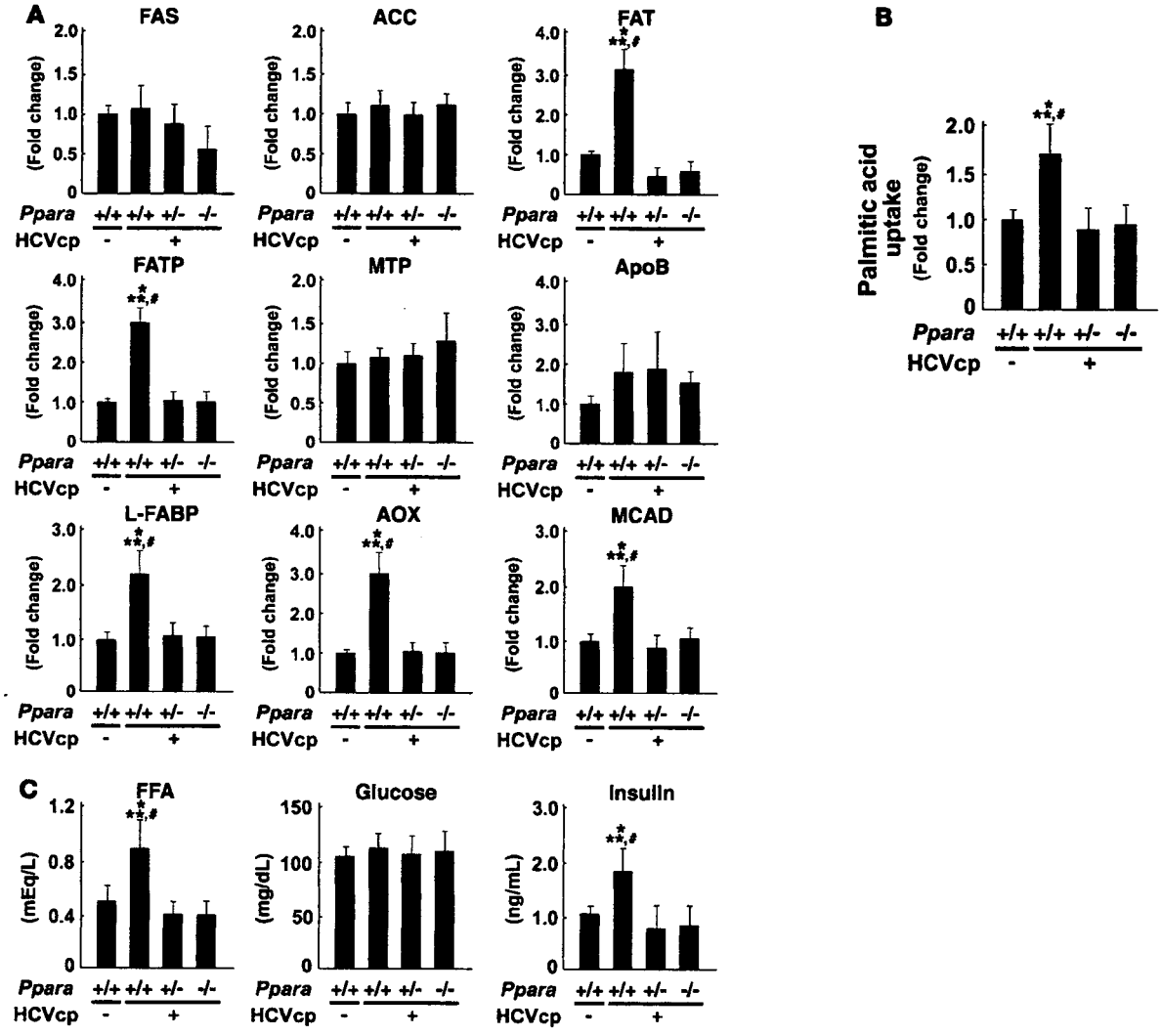

Figure 2

Analyses of factors associated with hepatic fatty acid and triglyceride metabolism. (**A**) Expression of genes associated with fatty acid and triglyceride metabolism in 9-month-old mouse livers. Total RNA was extracted from each mouse liver, and mRNA levels were determined by RT-PCR. mRNA levels were normalized by those of GAPDH and subsequently normalized by those in *Ppara*$^{+/+}$ nontransgenic mice. Results are expressed as the mean ± SD (n = 6/group). *P < 0.05 compared with *Ppara*$^{+/+}$ nontransgenic mice; **P < 0.05 compared with *Ppara*$^{+/-}$:HCVcpTg mice; #P < 0.05 compared with *Ppara*$^{-/-}$:HCVcpTg mice. (**B**) Uptake of fatty acids in 9-month-old mouse livers. Liver slices obtained from 3 mice in each group were incubated in medium containing 0.8 mM [1-^{14}C]palmitic acid for 7 h. Fatty acid uptake ability was estimated by the sum of palmitic acid converted to CO_2 and ketone bodies with that incorporated into total cellular lipids after incubation. The experiment was repeated 3 times. Results were normalized by those of *Ppara*$^{+/+}$ nontransgenic mice and expressed as the mean ± SD. (**C**) Plasma concentrations of free fatty acids, glucose, and insulin. After an overnight fast, blood was obtained from each mouse and the above variables were determined. Results are expressed as the mean ± SD (n = 6/group).

degeneration and necrosis, and fibrosis were not detected. On the other hand, *Ppara*$^{+/-}$:HCVcpTg and *Ppara*$^{-/-}$:HCVcpTg mice showed no steatosis (Figure 1, C and D). These results indicate that hepatic steatosis develops in *Ppara*$^{+/+}$:HCVcpTg mice, but not in *Ppara*$^{+/-}$:HCVcpTg and *Ppara*$^{-/-}$:HCVcpTg mice.

Hepatic fatty acid and triglyceride metabolism in transgenic mice. To investigate the mechanism responsible for the development of severe steatosis in *Ppara*$^{+/+}$:HCVcpTg mice, the expression of genes associated with fatty acid and triglyceride metabolism in the livers of 9-month-old mice was analyzed using the quantitative RT-PCR method. As shown in Figure 2A, the mRNA levels of genes related to de novo lipogenesis (fatty acid synthase [FAS] and acetyl-CoA carboxylase [ACC]) and secretion of VLDL (microsomal transfer protein [MTP] and apoB) were constant in all groups. The mRNA levels of fatty acid translocase (FAT) and fatty acid transport protein (FATP), which are associated with the uptake of fatty acids into hepatocytes, were significantly increased only in *Ppara*$^{+/+}$:HCVcpTg mice, but the mRNA levels of hepatic triglyceride lipase, another contributor to fatty acid uptake, remained unchanged (data not shown). The mRNA levels of liver fatty acid binding protein (L-FABP) were also elevated only in *Ppara*$^{+/+}$:HCVcpTg mice. Surprisingly, the mRNA levels of AOX and medium-chain acyl-CoA

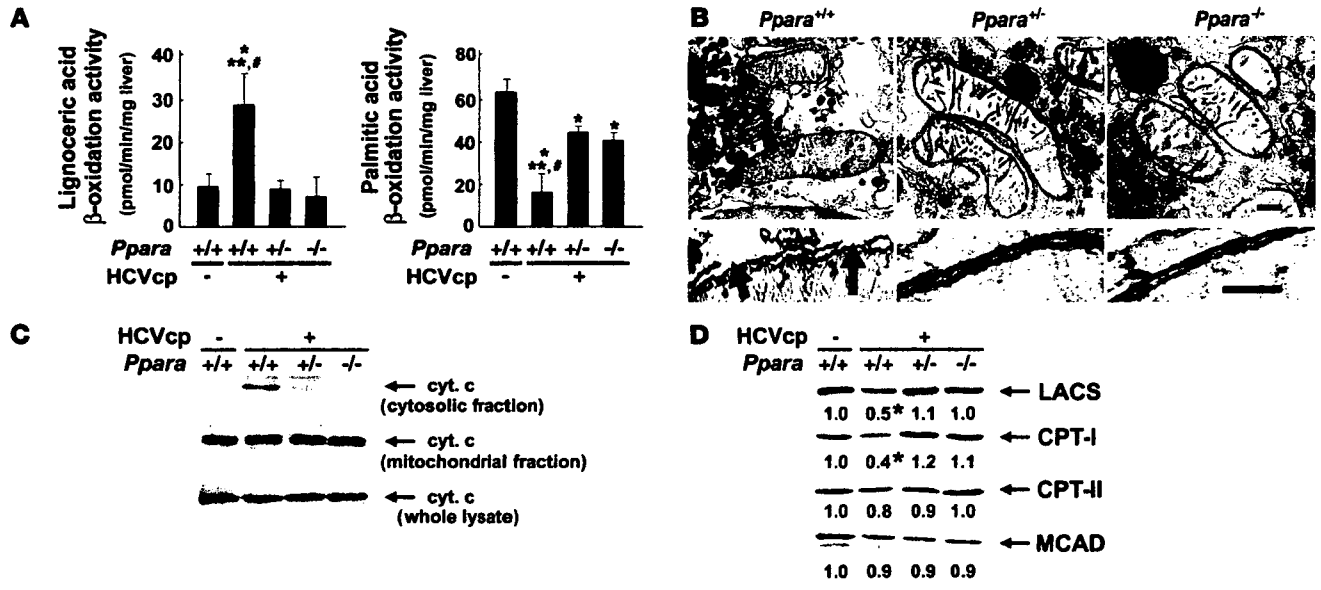

Figure 3

Analyses of mitochondrial abnormalities. (**A**) Lignoceric and palmitic acid β-oxidation activities in 9-month-old mice. Results are expressed as the mean ± SD (n = 6/group). *P < 0.05 compared with *Ppara*$^{+/+}$ nontransgenic mice; **P < 0.05 compared with *Ppara*$^{+/-}$:HCVcpTg mice; #P < 0.05 compared with *Ppara*$^{-/-}$:HCVcpTg mice. (**B**) Electron microscopic features of hepatic mitochondria of 9-month-old HCVcpTg mice. Upper and lower rows show a lower and higher magnification, respectively. In *Ppara*$^{+/+}$:HCVcpTg mice, some mitochondria showing discontinuance of outer membranes (arrows) and amorphous inner structures were observed. In *Ppara*$^{+/-}$:HCVcpTg and *Ppara*$^{-/-}$:HCVcpTg mice, mitochondria appeared normal; the scale bars represent 200 nm (top) and 30 nm (bottom), respectively. (**C**) Immunoblot analysis of cytochrome *c* in 9-month-old mice. Whole-liver lysate, mitochondrial fraction, or cytosolic fraction (50 μg protein) was loaded in each well. Results are representative of 4 independent experiments. (**D**) Immunoblot analysis of representative mitochondrial β-oxidation enzymes using a mitochondrial fraction prepared from 9-month-old mouse livers. The mitochondrial fraction (20 μg protein) was loaded in each well. Results are representative of 4 independent experiments. The band intensity was quantified densitometrically and normalized by that in *Ppara*$^{+/+}$ nontransgenic mouse. The mean value of the fold changes is shown under the representative band. LACS, long-chain acyl-CoA synthase; CPT, carnitine palmitoyl-CoA transferase.

dehydrogenase (MCAD), a rate-limiting enzymes in the peroxisomal and mitochondrial β-oxidation pathways, respectively, were significantly increased in *Ppara*$^{+/+}$:HCVcpTg mice. When fatty acid uptake ability was measured in fresh liver slices, it was significantly enhanced only in *Ppara*$^{+/+}$:HCVcpTg mice (Figure 2B). Additionally, plasma free fatty acid levels were higher in these mice than in mice in the other groups. Although there were no differences in fasting plasma glucose levels between the groups, hyperinsulinemia was observed only in *Ppara*$^{+/+}$:HCVcpTg mice (Figure 2C), in agreement with the previous observation that significant insulin resistance developed in these mice (8). Similar results were obtained from 24-month-old mice (data not shown). These results combined show that the increased plasma fatty acid levels, which were likely due to enhanced peripheral fatty acid release caused by insulin resistance, and the increase in fatty acid uptake ability are consistent with steatogenesis in *Ppara*$^{+/+}$:HCVcpTg mice.

Decreased mitochondrial β-oxidation in transgenic mice. Although the transcriptional activities of major β-oxidation enzymes were markedly increased, *Ppara*$^{+/+}$:HCVcpTg mice had severe steatosis. To explore this discrepant result, peroxisomal and mitochondrial β-oxidation activities were measured using lignoceric and palmitic acids as substrates, respectively. The lignoceric acid–degrading capacity was increased only in *Ppara*$^{+/+}$:HCVcpTg mice, where it corresponded to an increase in AOX expression. However, the capacity for palmitic acid degradation, which occurs particularly in mitochondria, was significantly lower in *Ppara*$^{+/+}$:HCVcpTg mice than in *Ppara*$^{+/-}$:HCVcpTg and *Ppara*$^{-/-}$:HCVcpTg mice (Figure 3A). Thus, decreased mitochondrial β-oxidation ability was considered to be another important mechanism for the development of steatosis induced by the core protein.

We further evaluated mitochondrial abnormalities. In electron microscopic examination, discontinuous outer membranes (Figure 3B, arrows) and lack of an internal structure were observed in some mitochondria of *Ppara*$^{+/+}$:HCVcpTg mouse livers, in agreement with the previous report (9). However, these abnormalities were not seen in *Ppara*$^{+/-}$:HCVcpTg and *Ppara*$^{-/-}$:HCVcpTg mice (Figure 3B). Immunoblot analysis showed that cytochrome *c*, which is usually localized in the mitochondrial intermembrane space, was present in the cytosolic fractions of *Ppara*$^{+/+}$:HCVcpTg mice (Figure 3C). Moreover, immunoblot analysis using mitochondrial fractions showed that the expression levels of long-chain acyl-CoA synthase and carnitine palmitoyl-CoA transferase-I, which are enzymes indispensable to the initial step of mitochondrial β-oxidation and are localized mainly in mitochondrial outer membranes, were significantly decreased only in *Ppara*$^{+/+}$:HCVcpTg mice (Figure 3D).

Overall, these results suggest that homozygous PPARα is essential to the pathogenesis of hepatic steatosis induced by the HCV core protein, which results from a decrease in mitochondrial fatty acid degradation capacity caused by the breakdown of mitochondrial outer membranes and a disproportionate increase in the uptake of fatty acids. Interestingly, steatosis and the related changes did not occur in *Ppara*$^{+/-}$ and *Ppara*$^{-/-}$ mice expressing the HCV core protein, which suggested that these changes were not caused by the core protein itself.

Table 1
Incidence of HCC in 24-month-old mice

HCV core protein	*Ppara*	Mice (*n*)	Mice with HCC (*n*)	Incidence (%)
–	+/+	20	0	0
–	+/–	18	0	0
–	–/–	20	0	0
+	+/+	17	6	35.3[A]
+	+/–	16	0	0
+	–/–	14	0	0

Mice were killed at 24 months of age for analysis. HCC was diagnosed according to histological findings. [A]$P < 0.05$ compared with *Ppara*$^{+/+}$ nontransgenic mice, $P < 0.05$ compared with *Ppara*$^{+/-}$:HCVcpTg mice, $P < 0.05$ compared with *Ppara*$^{-/-}$:HCVcpTg mice.

Requirement of homozygous PPARα for hepatic tumor development in transgenic mice. At 9 months of age, hepatic nodules were not observed at all in transgenic mice, whereas, at 24 months, approximately 35% of *Ppara*$^{+/+}$:HCVcpTg mice had macroscopically evident hepatic nodules (Table 1). Microscopically, these nodules had the appearance of well-differentiated HCC with trabecular features, which was consistent with the previous report (9). Surprisingly, *Ppara*$^{+/-}$:HCVcpTg and *Ppara*$^{-/-}$:HCVcpTg mice of the same ages developed no evidence of hepatic tumors, despite the expression of HCV core protein at similar levels to those found in *Ppara*$^{+/+}$:HCVcpTg mice (Table 1). Microscopic examination showed that there were no dysplastic cells or precancerous lesions throughout the livers in *Ppara*$^{+/-}$:HCVcpTg and *Ppara*$^{-/-}$:HCVcpTg mice (Figure 1C). These results provide strong evidence that homozygous PPARα is essential for hepatic tumorigenesis induced by HCV core protein.

Increased hepatocyte proliferation only in Ppara$^{+/+}$*:HCVcpTg mice.* Because sustained acceleration of hepatocyte proliferation relative to apoptosis may promote the development of HCC, these opposing processes were quantified in the livers of 24-month-old mice. Both the liver-to-body weight ratio and the number of hepatocytes expressing proliferating cell nuclear antigen (PCNA) were increased only in *Ppara*$^{+/+}$:HCVcpTg mice (Figure 4, A and B). In contrast, the number of TUNEL-positive hepatocytes and the hepatic caspase 3 activity, indicators of hepatocyte apoptosis, remained similar among the 3 mouse strains (Figure 4, C and D). Interestingly, despite the presence of HCV core protein, the amounts of these proliferative and apoptotic markers in *Ppara*$^{+/-}$:HCVcpTg and *Ppara*$^{-/-}$:HCVcpTg mice were similar to those in *Ppara*$^{+/+}$ nontransgenic mice. Expression levels of several proteins, such as protooncogenes (c-Fos and c-Myc), cell-cycle regulators (cyclin D1, cyclin-dependent kinase [CDK] 4, and PCNA), and phosphorylated ERK 1 and 2, all of which are associated with hepatocyte proliferation, were elevated in *Ppara*$^{+/+}$:HCVcpTg mice but not in other genotypes (Figure 4, E and F).

Increased oxidative stress and DNA damage only in Ppara$^{+/+}$*:HCVcpTg mice.* HCV core protein is associated with increased production of ROS (23). Enhanced ROS production induces nuclear DNA damage, which results in the initiation of hepatocarcinogenesis, and can also injure organelles, which can result in disorders in their

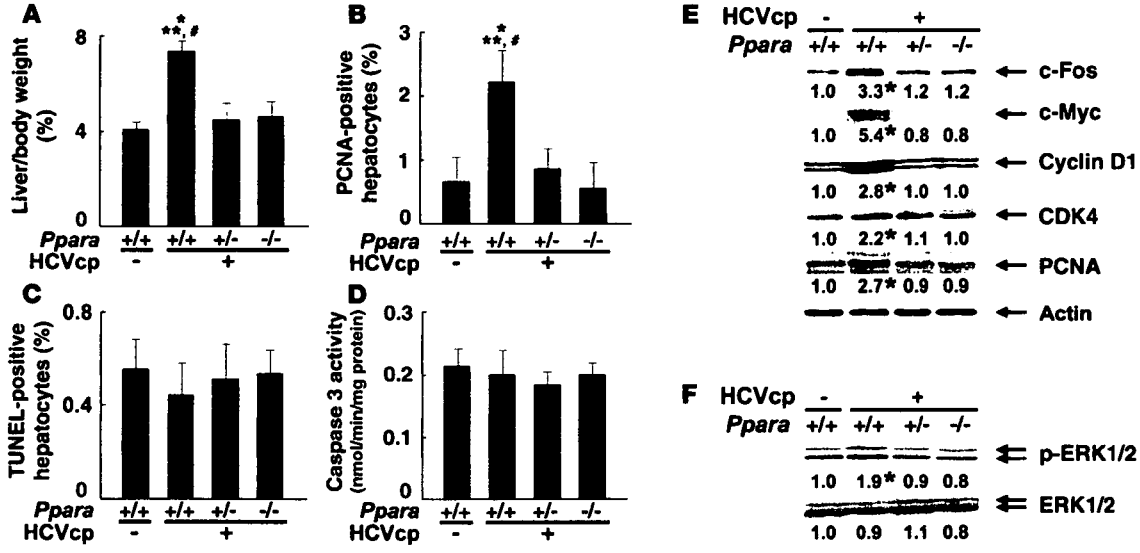

Figure 4
Increased hepatocyte proliferation in *Ppara*$^{+/+}$:HCVcpTg mice at 24 months of age. (**A**) Liver-to-body-weight ratio. Results are expressed as the mean ± SD (n = 6/group). (**B**) Numbers of proliferating hepatocytes. Two thousand hepatocytes were examined in each mouse, and hepatocyte nuclei positive for anti-PCNA antibody were counted. Results are expressed as the mean ± SD (n = 6/group). For **A** and **B**, comparisons are designated as follows: *$P < 0.05$ compared with *Ppara*$^{+/+}$ nontransgenic mice; **$P < 0.05$ compared with *Ppara*$^{+/-}$:HCVcpTg mice; #$P < 0.05$ compared with *Ppara*$^{-/-}$:HCVcpTg mice. (**C**) Numbers of apoptotic hepatocytes. Liver sections were subjected to TUNEL staining, and TUNEL-positive hepatocyte nuclei were counted in 2,000 hepatocytes from each mouse. Results are expressed as the mean ± SD (n = 6/group). (**D**) Caspase 3 activity. Results are expressed as the mean ± SD (n = 6/group). (**E**) Immunoblot analysis of oncogene products and cell cycle regulators. The same sample used in Figure 1A (whole-liver lysate, 50 μg protein) was loaded in each well. The band of actin was used as the loading control. Results are representative of 4 independent experiments. The band intensity was quantified densitometrically, normalized by that of actin, and subsequently normalized by that in *Ppara*$^{+/+}$ nontransgenic mice. The mean value of the fold changes is expressed under each band. (**F**) Immunoblot analysis of phosphorylated ERK1/2 and total ERK1/2. The same samples in Figure 4E (50 μg protein) were used.

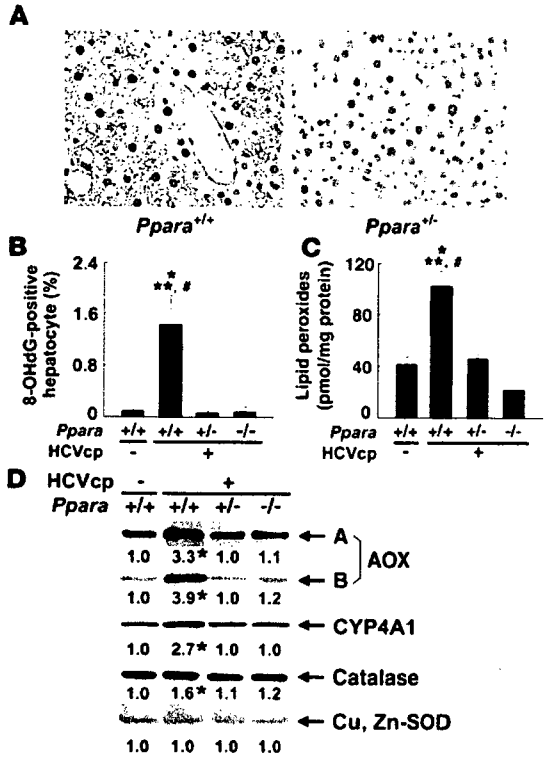

Figure 5

Increased oxidative stress and DNA damage in *Ppara*$^{+/+}$:HCVcpTg mice at 24 months of age. (**A**) Immunohistochemical staining using antibody against 8-OHdG. In *Ppara*$^{+/+}$:HCVcpTg mice, some steatotic hepatocytes were positive for 8-OHdG. Original magnification, ×400. (**B**) Numbers of 8-OHdG–positive hepatocytes. Hepatocyte nuclei stained with anti-8-OHdG antibody were counted in 2,000 hepatocytes of each mouse. Results are expressed as the mean ± SD (n = 6/group). (**C**) Hepatic content of lipid peroxides. Results are expressed as the mean ± SD (n = 6 /group). *P < 0.05 compared with *Ppara*$^{+/+}$ nontransgenic mice; **P < 0.05 compared with *Ppara*$^{+/-}$:HCVcpTg mice; #P < 0.05 compared with *Ppara*$^{-/-}$:HCVcpTg mice. (**D**) Immunoblot analysis of AOX, CYP4A1, catalase, and Cu, Zn-SOD. The whole-liver lysate used in the experiment in Figure 4E (20 μg protein for AOX and CYP4A1 and 50 μg for others) was loaded in each lane. The band of actin was used as the loading control. Results are representative of 4 independent experiments. **A** and **B** indicate full-length and truncated AOX, respectively. The band intensity was quantified densitometrically, normalized by that of actin, and subsequently normalized by that in *Ppara*$^{+/+}$ nontransgenic mice. The mean value of the fold changes is expressed under each band. *P < 0.05 compared with *Ppara*$^{+/+}$ nontransgenic mice.

function. The number of hepatocytes positive for 8-hydroxy-2′-deoxyguanosine (8-OHdG), an indicator of oxidative damage to nuclear DNA, was increased only in 24-month-old *Ppara*$^{+/+}$:HCVcpTg mice (Figure 5, A and B). Lipid peroxides were slightly increased in the livers of 9-month-old *Ppara*$^{+/+}$:HCVcpTg mice (data not shown) and were more abundant in the livers of 24-month-old *Ppara*$^{+/+}$:HCVcpTg mice than in those of *Ppara*$^{+/-}$:HCVcpTg and *Ppara*$^{-/-}$:HCVcpTg mice or *Ppara*$^{+/+}$ nontransgenic mice (Figure 5C). Expression of typical ROS-generating enzymes (AOX and cytochrome P450 4A1 [CYP4A1]) and ROS-eliminating enzymes (catalase and Cu, Zn-SOD) was examined. Immunoblot analysis showed marked increases in the expression of AOX and CYP4A1 and mild increases in that of catalase only in *Ppara*$^{+/+}$:HCVcpTg mice. No changes in Cu, Zn-SOD were found in the subgroups of transgenic mice (Figure 5D). These results suggest that enhanced oxidative stress causes damage in nuclear DNA and probably in mitochondria in the *Ppara*$^{+/+}$:HCVcpTg mice.

Persistent and spontaneous PPARα activation in Ppara$^{+/+}$*:HCVcpTg mice.* Liver tumorigenesis induced by long-term exposure to peroxisome proliferators and the related changes, such as sustained hepatocyte proliferation and increased oxidative stress, are associated with persistent PPARα activation (19–21). To examine the activation of PPARα, we quantified the level of PPARα mRNA, which is induced by PPARα activation (24, 25). PPARα mRNA levels were higher in 9-month-old *Ppara*$^{+/+}$:HCVcpTg mice than in *Ppara*$^{+/+}$ nontransgenic mice (Figure 6A). These increases were more pronounced at 24 months of age. However, there were no differences in PPARα mRNA levels between *Ppara*$^{+/-}$:HCVcpTg and *Ppara*$^{+/-}$ nontransgenic mice at either 9 or 24 months of age. The expression levels of typical PPARα target genes (16, 25, 26) — such as FAT, FATP, L-FABP, AOX, and MCAD (Figure 2); c-Myc, cyclin D1, CDK4, and PCNA (Figure 4); and CYP4A1 (Figure 5) — were simultaneously and synchronously increased in *Ppara*$^{+/+}$:HCVcpTg mice, but not in *Ppara*$^{+/-}$:HCVcpTg or *Ppara*$^{-/-}$:HCVcpTg mice. These results confirm that persistent activation of PPARα occurs only in *Ppara*$^{+/+}$:HCVcpTg mice. Various changes observed in *Ppara*$^{+/+}$:HCVcpTg mice, i.e., increased fatty acid uptake, mitochondrial abnormalities, steatosis, ROS overproduction, accelerated hepatocyte proliferation, and hepatocarcinogenesis, were considered to be closely linked with sustained PPARα activation.

Nuclear PPARα content. The results described above suggest that persistent PPARα activation is critical to the steatogenesis and hepatocarcinogenesis induced by the HCV core protein. A question arises as to why *Ppara*$^{+/-}$:HCVcpTg mice with an active *Ppara* allele do not exhibit the hallmarks of PPARα activation and do not develop HCC. To address this issue, the nuclear PPARα content was analyzed. Immunoblot analysis for PPARα showed that the amount of nuclear PPARα protein in *Ppara*$^{+/+}$:HCVcpTg mice was approximately 2- to 3-fold that of *Ppara*$^{+/+}$ nontransgenic mice, which was disproportionate to the higher PPARα mRNA levels (approximately 1.2- to 1.6-fold) (Figure 6, A and B). The level of nuclear PPARα in *Ppara*$^{+/-}$:HCVcpTg mice was significantly lower than that in *Ppara*$^{+/+}$:HCVcpTg mice and was similar to that in *Ppara*$^{+/+}$ nontransgenic mice (Figure 6B). Thus, the lower amount of nuclear PPARα in *Ppara*$^{+/-}$:HCVcpTg mice than in *Ppara*$^{+/+}$:HCVcpTg mice might have heightened the threshold of expression required for long-term spontaneous PPARα activation.

The degree of an increase in nuclear PPARα levels was evidently higher than the degree of an increase in PPARα mRNA levels in HCVcpTg mice (Figure 6, A and B). To investigate this disparity, the stability of nuclear PPARα was evaluated by pulse-chase experiments using isolated hepatocytes obtained from these mice. The half-life of nuclear PPARα was significantly longer (P < 0.05) in *Ppara*$^{+/+}$:HCVcpTg mice (11.5 ± 2.3 h) than in *Ppara*$^{+/+}$ nontransgenic mice (5.8 ± 1.4 h) (Figure 6C). The half-life of nuclear PPARα in *Ppara*$^{+/-}$:HCVcpTg mice tended to be prolonged compared with that in *Ppara*$^{+/-}$ nontransgenic mice (Figure 6C). These results suggest that the stability of nuclear PPARα was increased as a result of HCV core protein expression. Because it is known that the core protein interacts with retinoid X receptor α (RXRα) (27) and that

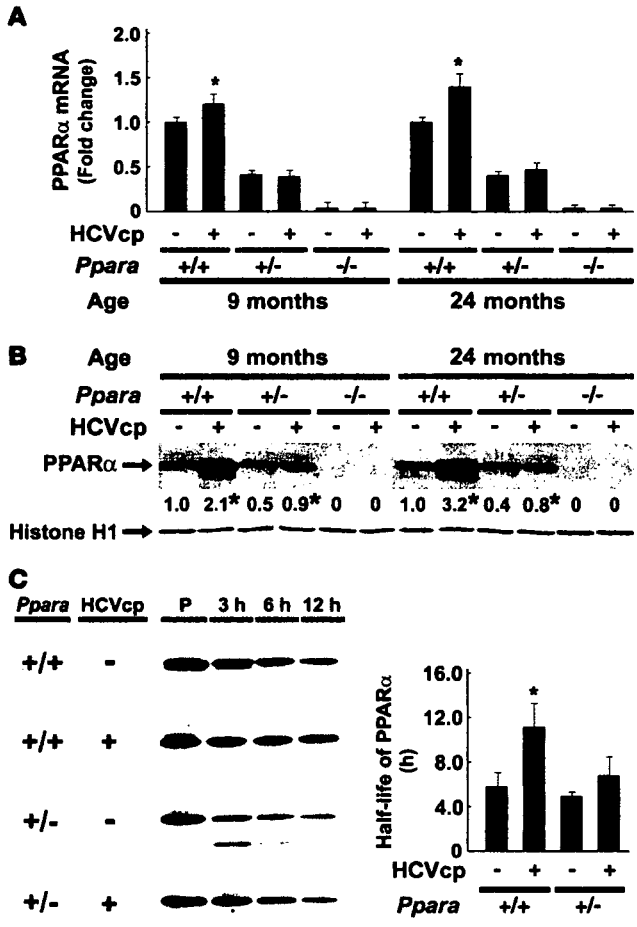

Figure 6

Persistent PPARα activation in *Ppara*$^{+/+}$:HCVcpTg mice. (**A**) PPARα mRNA levels. Total RNA was prepared from each mouse, and PPARα mRNA levels were determined by RT-PCR, normalized by those of GAPDH, and subsequently normalized by those of 9-month-old *Ppara*$^{+/+}$ nontransgenic mice. Results are expressed as the mean ± SD (n = 6 /group). (**B**) Immunoblot analysis of nuclear PPARα. The nuclear fraction obtained from each mouse (100 μg protein) was loaded in each well. The band of histone H1 was used as the loading control. Results are representative of 6 independent experiments. The band intensity was quantified densitometrically, normalized by that of histone H1, and subsequently normalized by that in 9-month-old *Ppara*$^{+/+}$ nontransgenic mice. The mean value is expressed under each band. *P < 0.05 compared with nontransgenic mice of the same age and *Ppara* genotype. (**C**) Pulse-chase experiments for 3, 6, and 12 h and pulse-label (P) experiments for nuclear PPARα using isolated mouse hepatocytes. Left: labeled PPARα bands on x-ray film. Pulse-label and pulse-chase experiments were performed as described in Methods. Results are representative of 4 independent experiments. Right: half-life of PPARα. The band intensity was measured densitometrically and subsequently normalized by that of the pulse-label experiments. The percentage of the band intensity was plotted, and the half-life of PPARα was calculated. Results obtained from 4 independent experiments are expressed as the mean ± SD. *P < 0.05 compared with nontransgenic mice in the same *Ppara* genotype.

PPARα influences the stability of RXRα (28), it is plausible that the core protein would affect its action in nuclei through an interaction with the PPARα-RXRα heterodimer and stabilization of PPARα.

Development of hepatic steatosis and HCC with long-term clofibrate treatment in Ppara$^{+/-}$*:HCVcpTg mice.* To further confirm the significance of persistent PPARα activation on core protein–induced pathological changes, *Ppara*$^{+/-}$ and *Ppara*$^{+/-}$:HCVcpTg mice were fed a standard diet containing 0.05% clofibrate for 24 months. Interestingly, hepatic steatosis appeared in the clofibrate-treated *Ppara*$^{+/-}$:HCVcpTg mice, but not in the *Ppara*$^{+/-}$ mice under the same treatment conditions (Figure 7, A and B). Similar to our observations in *Ppara*$^{+/+}$:HCVcpTg mice not treated with clofibrate, aberrant mitochondria with discontinuous outer membranes and decreased palmitic acid β-oxidation activity were found only in the clofibrate-treated *Ppara*$^{+/-}$:HCVcpTg mice (Figure 7, A and C). In addition, levels of MCAD mRNA; AOX, and CYP4A1 proteins; PPARα mRNA; and nuclear PPARα protein were higher in the clofibrate-treated *Ppara*$^{+/-}$:HCVcpTg mice than in the clofibrate-treated *Ppara*$^{+/-}$ mice (Figure 7, D–F), which suggests that the degree of PPARα activation in the former group was greater than that in the latter group and similar to that in *Ppara*$^{+/+}$:HCVcpTg mice not treated with clofibrate. Finally, the incidence of HCC after clofibrate treatment was higher in *Ppara*$^{+/-}$:HCVcpTg mice (25%; 5 in 20 mice) than in *Ppara*$^{+/-}$ mice (5%; 1 in 20 mice). Therefore, these results corroborate the importance of constant PPARα activation to the pathogenesis of hepatic steatosis and HCC in the transgenic mice.

Discussion

A novel and striking finding in this study is the absolute requirement of persistent PPARα activation for the development of HCV core protein–induced steatosis and HCC. Our data also show that the HCV core protein alone cannot induce steatosis and HCC in transgenic mice.

Mechanisms of development of steatosis in HCVcpTg mice were previously explained as an enhancement of de novo synthesis of fatty acids (29) and a decrease in MTP expression, the latter of which results in insufficient VLDL secretion from hepatocytes (30). In the present study, we revealed 2 novel mechanisms of steatogenesis in the transgenic mice, i.e., an impairment of mitochondrial β-oxidation due to the breakdown of mitochondrial outer membranes and an increase in fatty acid uptake into hepatocytes, associated with PPARα activation. PPARα activation, mitochondrial dysfunction, and hepatic steatosis appeared in 9-month-old *Ppara*$^{+/+}$:HCVcpTg mice and continued until 24 months of age, clearly preceding development of HCC. These findings thereby indicate a correlation between PPARα activation, hepatic steatosis, and HCC.

We obtained the novel and rather paradoxical finding that significant PPARα activation, which generally is expected to reduce hepatic triglyceride levels, is essential for the development of severe steatosis induced by HCV core protein. According to the results of this study, the following hypothesis concerning the development of steatosis in *Ppara*$^{+/+}$:HCVcpTg mice is proposed. First, the HCV core protein localizes partly in mitochondria (9). A recent study

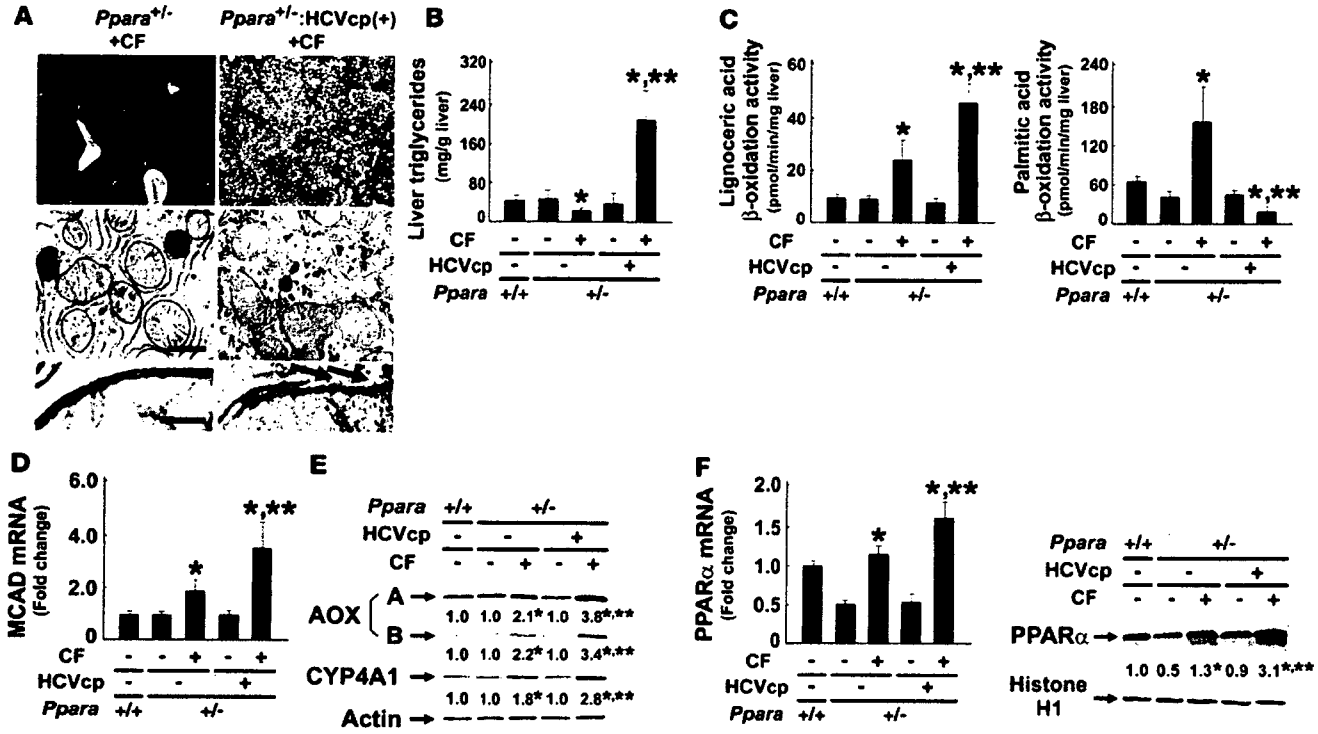

Figure 7

Development of hepatic steatosis by long-term treatment of clofibrate in *Ppara*$^{+/-}$:HCVcpTg mice. (**A**) Histological examination of *Ppara*$^{+/-}$ and *Ppara*$^{+/-}$:HCVcpTg mice treated with diet containing 0.05% (w/w) clofibrate for 24 months (CF). Top: Histological appearance of H&E-stained liver sections. Magnification, ×40. Microvesicular and macrovesicular steatosis were detected only in clofibrate-treated *Ppara*$^{+/-}$:HCVcpTg mice. Middle and bottom: Electron microscopic features of hepatic mitochondria. Some C-shaped mitochondria showing discontinuance of outer membranes (arrows) were found in clofibrate-treated *Ppara*$^{+/-}$:HCVcpTg mice. Scale bars: 400 nm (middle), 30 nm (bottom). (**B** and **C**) Content of liver triglycerides and lignoceric and palmitic acid β-oxidation activities. (**D**) MCAD mRNA levels. mRNA levels were normalized to those of GAPDH and subsequently normalized to those in *Ppara*$^{+/+}$ nontransgenic mice. (**E**) Immunoblot analysis of AOX and CYP4A1. Whole-liver lysate (20 μg protein) was loaded in each lane. Actin was used as a loading control. Results are representative of 6 independent experiments. (**F**) PPARα mRNA levels and nuclear PPARα contents. Left: PPARα mRNA levels. The same samples used in **D** were adopted. Right: Immunoblot analysis of nuclear PPARα. Nuclear fraction obtained from each mouse (100 μg protein) was loaded in each well. Histone H1 was used as a loading control. In **E** and **F**, the mean value of the fold changes is shown under each band. Results are representative of 6 independent experiments. Band intensity was quantified densitometrically, normalized to that of the loading control, and subsequently normalized to that in *Ppara*$^{+/+}$ nontransgenic mice. $^{*}P < 0.05$ compared with untreated mice of the same genotype; $^{**}P < 0.05$ compared with clofibrate-treated *Ppara*$^{+/-}$ mice without core protein gene. Results are expressed as mean ± SD (n = 6/group).

showed that, in isolated mitochondria, the core protein directly increased Ca^{2+} influx, inhibited electron transport complex I activity, and induced ROS production (31), all of which can increase the fragility of mitochondria and depress mitochondrial function. In addition, the HCV core protein also localizes in nuclei (9) and can coexist in PPARα-RXRα heterodimer through a direct interaction with the DNA-binding domain of RXRα, which enhances the transcriptional activity of PPARα target genes, such as AOX, despite the absence of PPARα ligands in cultured cells (27). The HCV core protein can also be involved in the PPARα-RXRα complex through a direct interaction with cyclic-AMP responsive element binding protein-binding protein (32), which is able to bind to PPARα (33). Thus, the core protein probably serves as a coactivator and stabilizer of PPARα in vivo, which was further confirmed in this study. Moreover, because it is also known that the core protein itself activates ERK1/2 and p38 mitogen-activated protein kinase (34), these activations might phosphorylate PPARα and thereby transactivate it (35). The core protein–induced PPARα activation enhances the basal expression of AOX and CYP4A1, which leads to increased production of ROS and dicarboxylic acids. These toxic compounds can damage mitochondrial outer membranes, which impairs the mitochondrial β-oxidation system. These damages directly induce the accumulation of long-chain fatty acids in hepatocytes. Furthermore, PPARα activation increases the expression of FAT and FATP, which promotes the influx of fatty acids from blood. Long-chain fatty acids and their CoA esters accumulated in hepatocytes are likely to act as potent detergents, which further damages the outer membranes of mitochondria. Fatty acids and their derivatives function as natural ligands of PPARα, which results in the activation of PPARα and the induction of FAT, FATP, AOX, and CYP4A1, which further accelerates mitochondrial damage, the reduction of mitochondrial β-oxidation activity, and the accumulation of fatty acids in a vicious cycle.

Persistent PPARα activation increases oxidative DNA damage because of a disproportionate increase in ROS-generating enzymes relative to the levels of degrading enzymes such as catalase and SOD, which can predispose hepatocytes to malignant transformation. In addition, persistent PPARα activation leads to increased

Table 2
Primer pairs used for RT-PCR

Gene	GeneBank accession number		Primer sequence	Product (bp)
ACC	NM_133360	F	5′-GGGCACAGACCGTGGTAGTT-3′	105
		R	5′-CAGGATCAGCTGGGATACTGAGT-3′	
ApoB	NM_009693	F	5′-TCACCCCCGGGATCAAG-3′	85
		R	5′-TCCAAGGACACAGAGGGCTTT-3′	
AOX	NM_015729	F	5′-TGGTATGGTGTCGTACTTGAATGAC-3′	145
		R	5′-AATTTCTACCAATCTGGCTGCAC-3′	
FAS	NM_007988	F	5′-ATCCTGGAACGAGAACACGATCT-3′	140
		R	5′-AGAGACGTGTCACTCCTGGACTT-3′	
FAT	NM_007643	F	5′-CCAAATGAAGATGAGCATAGGACAT-3′	87
		R	5′-GTTGACCTGCAGTCGTTTTGC-3′	
FATP	NM_011977	F	5′-ACCACCGGGCTTCCTAAGG-3′	80
		R	5′-CTGTAGGAATGGTGGCCAAAG-3′	
GAPDH	M32599	F	5′-TGCACCACCAACTGCTTAG-3′	177
		R	5′-GGATGCAGGGATGATGTTCTG-3′	
L-FABP	NM_017399	F	5′-GCAGAGCCAGGAGAACTTTGAG-3′	121
		R	5′-TTTGATTTTCTTCCCTTCATGCA-3′	
MCAD	NM_007382	F	5′-TGCTTTTGATAGAACCAGACCTACAGT-3′	128
		R	5′-CTTGGTGCTCCACTAGCAGCTT-3′	
MTP	NM_008642	F	5′-GAGCGGTCTGGATTTACAACG-3′	72
		R	5′-GTAGGTAGTGACAGATGTGGCTTTTG-3′	
PPARα	NM_011144	F	5′-CCTCAGGGTACCACTACGGAGT-3′	69
		R	5′-GCCGAATAGTTCGCCGAA-3′	

F, forward sequence; R, reverse sequence.

cell division, as revealed by the expression of cell cycle regulators such as cyclin D1 and CDK4. Furthermore, there is little change in apoptosis, which, under normal circumstances, would remove damaged cells capable of undergoing transformation. Thus, under these conditions, it is plausible that some aberrant hepatocytes do not undergo apoptosis and develop into HCC.

It is well known that chronic activation of PPARα is associated with hepatocarcinogenesis in mice exposed to peroxisome proliferators or in mice lacking AOX expression. The common clinicopathological characteristics of HCC in these mice are multicentric HCC (20, 22, 36, 37), the well-differentiated appearance of HCC including trabecular features and often a "nodule-in-nodule" pattern (22, 36, 37), and no evidence of fibrosis or cirrhosis in the nonneoplastic liver parenchyma (22, 36), similar to that observed in *Ppara*$^{+/+}$:HCVcpTg mice. However, mice chronically exposed to peroxisome proliferators are clearly distinct from *Ppara*$^{+/+}$:HCVcpTg mice in that they have normal mitochondrial organization, increased mitochondrial β-oxidation activity, and no steatosis (16, 36). AOX-null mice are also different from *Ppara*$^{+/+}$:HCVcpTg mice with respect to mitochondrial structure (22). These detailed comparisons between the 3 mouse models reveal the importance of mitochondrial abnormalities in the pathogenesis of HCV-related diseases.

PPARα is known to regulate the hepatic expression of many proteins associated with fatty acid and triglyceride metabolism, cell division and apoptosis, oxidative stress generation and degradation, and so forth (15, 16, 20, 21, 24–26); therefore, complete deletion of the PPARα gene from mice might cause hitherto unknown influences on the pathways involved in the development of hepatic steatosis and HCC. To consider these unknown effects, *Ppara*$^{+/-}$:HCVcpTg mice were adopted in the current study. Surprisingly, almost all results from *Ppara*$^{+/-}$:HCVcpTg mice were similar to those from *Ppara*$^{-/-}$:HCVcpTg mice, which demonstrates that the presence of functional PPARα itself is not a prerequisite for the occurrence of steatosis and HCC induced by the HCV core protein. Moreover, a comparison between *Ppara*$^{+/-}$:HCVcpTg and *Ppara*$^{+/+}$:HCVcpTg mice uncovered an unexpected and important fact that the core protein–dependent pathological changes do not appear without significant activation of PPARα. Thus, it is not the presence of PPARα per se, but rather a high level of PPARα activation that seems to be essential for the development of HCV core protein–induced steatosis and HCC.

To reinforce the abovementioned hypothesis, *Ppara*$^{+/-}$ and *Ppara*$^{+/-}$:HCVcpTg mice were treated with an exogenous PPAR agonist, clofibrate, for 24 months. In *Ppara*$^{+/-}$ mice, long-term clofibrate treatment caused a certain level of persistent PPARα activation and a low incidence of HCC. Interestingly, in *Ppara*$^{+/-}$:HCVcpTg mice, clofibrate treatment induced more intensive PPARα activation and HCC at a much higher incidence, accompanied by damaged mitochondrial outer membranes, severe steatosis, and decreased mitochondrial β-oxidation activity. The results from the clofibrate-treated *Ppara*$^{+/-}$:HCVcpTg mice were similar to those of the *Ppara*$^{+/+}$:HCVcpTg mice not treated with clofibrate. Therefore, these findings further support the concept that a long-term and high level of PPARα activation is necessary for steatogenesis and hepatocarcinogenesis in HCVcpTg mice and emphasize the significant role of the HCV core protein as a PPARα coactivator in vivo.

A pulse-chase experiment showed that PPARα was stabilized in hepatocyte nuclei in mice expressing the HCV core protein. Many nuclear receptors, including PPARα and RXRα, are known to be degraded by the ubiquitin-proteasome system (38), which plays an important role in modulating the activity of nuclear receptors. Further studies will be needed to clarify whether the core protein influences the ubiquitin-proteasome pathway.

Recent studies have shown conflicting result, i.e., that PPARα was downregulated in the livers of chronic hepatitis C patients (39, 40). Although the association between PPARα function and chronic HCV infection remains a matter of controversy in humans, the changes observed in the transgenic mice resemble in many ways the clinicopathological features of chronically HCV-infected patients; both show a high frequency of accompanying steatosis (10, 40, 41), increased accumulation of carbon 18 monounsaturated fatty acids in the liver (42), mitochondrial dysfunction (43), increased insulin resistance (44) and oxidative stress (45, 46), male-preferential (2) and multicentric occurrence of HCC (47, 48), and the well-differentiated appearance of HCC, including trabecular features and often a "nodule-in-nodule" pattern (47, 48). Thus, it is postulated that the mechanism of steatogenesis and hepatocarcinogenesis we proposed may partially apply to patients with chronic HCV infection. If so, therapeutic interventions to alleviate persistent and excessive PPARα activation might be beneficial in the prevention of HCC. To clarify the exact relationship between PPARα activation and HCV-induced hepatocarcinogenesis in humans, further

experiments using noncancerous liver tissues obtained from HCV-related HCC patients and using mice carrying human PPARα and HCV core protein genes are needed.

In conclusion, we clarified for the first time that persistent and potent PPARα activation is absolutely required for the development of severe steatosis and HCC induced by HCV core protein. In addition, we uncovered paradoxical and specific functions of PPARα in the mechanism of steatogenesis mediated by the core protein. Our results offer clues in the search for novel therapeutic and nutritional management options, especially with respect to neutral lipids, for chronically HCV-infected patients.

Methods

Mice. The generation of HCVcpTg mice and *Ppara*$^{-/-}$ mice was described previously (7, 24, 49). Male HCVcpTg mice and female *Ppara*$^{-/-}$ mice were mated, and F1 mice bearing the HCV core protein gene were intercrossed to produce F2 mice. *Ppara*$^{+/+}$, *Ppara*$^{+/-}$, and *Ppara*$^{-/-}$ mice bearing the HCV core protein gene, designated as *Ppara*$^{+/+}$:HCVcpTg, *Ppara*$^{+/-}$:HCVcpTg, and *Ppara*$^{-/-}$:HCVcpTg mice, in the F4 generation were subjected to serial analyses. Because HCC develops preferentially in male HCVcpTg mice (9), male mice were analyzed. Age-matched male *Ppara*$^{+/+}$ mice without the core protein gene were used as controls. For identifying genotypes, genomic DNA was isolated from mouse tails and amplified by PCR. Primer pairs were designed as described elsewhere: 5′-GCCCACAGGACGTTAAGTTC-3′ and 5′-TAGTTCACGCCGTCCTCCAG-3′ for the HCV core gene (7) and 5′-CAGAGCAACCATCCAGATGA-3′ and 5′-AAACGCAACGTAGAGTGCTG-3′ for the PPARα gene (24). Amplified alleles for HCV core and PPARα genes were 460 and 472 base pairs, respectively. Five mice per cage were fed a routine diet and were kept free of specific pathogens according to institutional guidelines. For the clofibrate treatment experiments, 2-month-old male *Ppara*$^{+/-}$ and *Ppara*$^{+/-}$:HCVcpTg mice were randomly divided into 2 groups (n = 20 in each group) and were fed either a routine diet or one containing 0.05% (w/w) clofibrate (Wako Pure Chemicals Industries) for 24 months. All mice were killed by cervical dislocation before their livers were excised. If a hepatic tumor was present, the tumor was removed and subjected to histological analysis, and the remaining liver tissues were used for biochemical analyses. All animal experiments were conducted in accordance with animal study protocols outlined in the *Guide for the Care and Use of Laboratory Animals* prepared by the National Academy of Sciences and approved by the Shinshu University School of Medicine.

Preparation of nuclear, mitochondrial, and cytosolic fractions. Approximately 400 mg of liver tissue was minced on ice and transferred to 10% (w/v) isolation buffer (250 mM sucrose in 10 mM Tris-HCl [pH 7.4] and 0.5 mM EGTA and 0.1% bovine serum albumin [pH 7.4]). The samples were gently homogenized by 10–20 strokes with a chilled Dounce homogenizer (Wheaton) and loose-fitting pestle. The homogenate was centrifuged at 500 × *g* for 5 min at 4°C. The supernatant was retained, and the resulting pellet was resuspended with isolation buffer and centrifuged at 4,500 *g* for 10 min at 4°C. The pellet fraction was suspended again and centrifuged at 20,000 × *g* for 1 h at 4°C, and the resulting pellet was used as the nuclear fraction. The combined supernatant fractions were centrifuged at 7,800 × *g* for 10 min at 4°C to obtain a crude mitochondria pellet. This pellet was resuspended with isolation buffer, centrifuged at 7,800 × *g* for 10 min at 4°C, and used as the mitochondrial fraction. Finally, all supernatant fractions were collected and centrifuged at 20,000 × *g* for 30 min at 4°C, and the resulting supernatant was used as the cytosolic fraction.

Immunoblot analysis. Protein concentrations were measured colorimetrically with a BCA Protein Assay kit (Pierce). For the analysis of fatty acid–metabolizing enzymes, hepatocyte mitochondrial fractions or whole-liver lysates (20 μg protein) were subjected to 10% SDS-PAGE (16). For analysis of PPARα, nuclear fractions (100 μg protein) were used. For analysis of other proteins, whole lysates or cytosolic fractions (50 μg protein) were subjected to electrophoresis. After electrophoresis, the proteins were transferred to nitrocellulose membranes, which were incubated with the primary antibody and then with alkaline phosphatase-conjugated goat anti-rabbit or anti-mouse IgG. Antibodies against HCV core protein, fatty acid–metabolizing enzymes, CYP4A1, catalase, and PPARα were described previously (9, 16, 24, 50). Antibodies against other proteins were purchased commercially: cytochrome *c* antibody from BD Transduction Laboratories and other antibodies from Santa Cruz Biotechnology. The band of actin or histone H1 was used as the loading control. The band intensity was measured densitometrically, normalized to that of actin or histone H1, and subsequently expressed as fold changes relative to that of *Ppara*$^{+/+}$ nontransgenic mice.

Analysis of mRNA. Total liver RNA was extracted using an RNeasy Mini Kit (Qiagen), and cDNA was generated by SuperScript II reverse transcriptase (Gibco BRL). Quantitative RT-PCR was performed using a SYBR green PCR kit and an ABI Prism 7700 Sequence Detection System (Applied Biosystems). The primer pairs used for RT-PCR are shown in Table 2. The mRNA level was normalized to the GAPDH mRNA level and subsequently expressed as fold changes relative to that of *Ppara*$^{+/+}$ nontransgenic mice.

Light microscopy and immunohistochemical analysis. Small blocks of liver tissue from each mouse were fixed in 10% formalin in phosphate-buffered saline and embedded in paraffin. Sections (4 μm thick) were stained with hematoxylin and eosin. For immunohistochemical localization of PCNA and 8-OHdG, other small blocks of liver tissue were fixed in 4% paraformaldehyde in phosphate-buffered saline. Sections (4 μm thick) then were affixed to glass slides and incubated overnight with mouse monoclonal antibodies against PCNA (1:100 dilution; Santa Cruz) or 8-OHdG (1:10 dilution; Japan Institute for the Control of Aging). Sections were immunostained using EnVision+ kit, with 3,3′-diaminobenzidine as a substrate (DAKO). Hepatocytes positive for PCNA or 8-OHdG were examined in 10 randomly selected ×400 microscopic fields per section. Two-thousand hepatocytes were examined for each mouse, and the number of immunostained hepatocyte nuclei was expressed as a percentage.

Assessment of hepatocyte apoptosis. TUNEL assay was performed using a MEBSTAIN Apoptosis Kit II (Medical & Biological Laboratories). Two thousand hepatocytes were examined for each mouse, and the number of TUNEL-positive hepatocytes was expressed as a percentage.

Pulse-label and pulse-chase experiments. Parenchymal hepatocytes were isolated by the modified *in situ* perfusion method (51). After perfusion with 0.05% collagenase solution (Wako), the isolated hepatocytes were washed 3 times by means of differential centrifugation and the dead cells were removed by density-gradient centrifugation at 500 *g* for 3 min at 4°C on Percoll (Amersham Pharmacia Biotech). The live hepatocytes were washed and suspended in William's E medium containing 5% FBS. When the viability of the isolated hepatocytes exceeded 85% as determined by the trypan blue exclusion test, the following experiments were conducted. The isolated hepatocytes were washed twice and incubated in methionine-free medium containing 5% dialyzed FBS for 1 h at 37°C. The medium was replaced with the same medium containing 300 mCi/ml of [^{35}S]methionine (Amersham Pharmacia Biotech). After a 3-h incubation, the labeled medium was exchanged for the standard medium, and the preparation was chased for 3, 6, or 12 h. The labeled cells were washed, homogenized, and centrifuged at 800 *g* for 5 min at 4°C to obtain a crude nucleus pellet. This pellet was resuspended with isolation buffer and centrifuged at 20,000 *g* for 1 h at 4°C to prepare the nuclear fraction. The levels of radioactivity in the homogenates of the pulse-labeled preparations were similar between the transgenic and the nontransgenic mice, which suggested that the [^{35}S]methionine uptake capacity in the former hepatocytes was similar to that in the latter. The nuclear fraction was lysed in RIPA buffer (10 mM Tris-HCl, pH 7.4; 0.2% sodium deoxycholate, 0.2% Nonidet P-40, 0.1% SDS,

0.25 mM PMSF, and 10 mg/ml aprotinin). The lysate was incubated for 3 h at 4°C with purified anti-PPARα antibody. The immune complexes were precipitated with *Staphylococcus aureus* protein A bound to agarose beads. After the precipitates had been washed in RIPA buffer, the labeled proteins were resolved by 10% SDS-PAGE and visualized by autoradiography.

Analysis of fatty acid uptake ability. Assays for fatty acid uptake were carried out according to a method reported by Graulet et al. (52) with minor modifications. Briefly, 3 mice in each group were fasted overnight. Livers were removed quickly, rinsed in ice-cold saline solution, and cut into 500-μm thick slices with an Oxford Vibratome (Oxford Laboratories). Approximately 150 mg of fresh liver (6–8 liver slices) was placed on stainless steel grids positioned in a 25-ml flask equipped with suspended plastic center wells (Kontes) and incubated in RPMI-1640 medium (Sigma-Aldrich) devoid of fatty acids for 2 h at 37°C. The medium was then replaced with fresh RPMI-1640 medium supplemented with an antibiotic-antimycotic cocktail and 0.8 mM [1-^{14}C]palmitic acid (4 mCi/mmol) (American Radiolabeled Chemicals) complexed to BSA (palmitic acid:albumin molar ratio of 4:1). After a 7-h incubation, the medium was collected and slices were washed with 2 ml of saline solution and homogenized in Tris buffer (25 mM Tris-HCl, pH 8.0; 50 mM NaCl). Fatty acid uptake ability was calculated as the sum of palmitic acid converted to CO_2 and ketone bodies with that incorporated into total cellular lipids after incubation. For measurement of CO_2 production by the liver slices, the center wells were placed into scintillation vials containing 4 ml of scintillation cocktail, and radioactivity was counted. For measurement of ketone body generation, aliquots of medium (500 μl) and liver homogenates (250 μl) were treated with ice-cold perchloric acid to make final concentrations of 200 mM and were centrifuged at 3,000 *g* for 20 min at 4°C. Aliquots of the supernatant containing the ketone bodies were introduced into the scintillation vials, and radioactivity was counted. Total cellular lipids were extracted from the liver homogenates according to a modified method developed by Folch et al. (53), collected into scintillation vials, and evaporated to dryness under an air stream; radioactivity was then counted. The experiment was repeated 3 times, and palmitic acid uptake ability was expressed as fold changes relative to that of *Ppara*$^{+/+}$ nontransgenic mice.

Other methods. To determine the hepatic content of lipids and lipid peroxides, lipids were extracted according to a method by Folch et al. (53). Triglycerides and free fatty acids were measured with a Triglyceride E-test kit and a NEFA C-test kit (Wako), respectively. Lipid peroxides (malondialdeyde and 4-hydroxyalkenals) were measured using an LPO-586 kit (OXIS International). Hepatic β-oxidation activity was determined as described previously (16). Hepatic caspase 3 activity was measured as described elsewhere (54). Plasma glucose and insulin levels were determined using a Glucose CII-test kit (Wako) and a mouse insulin ELISA kit (U-type, AKRIN-031; Shibayagi), respectively.

Statistics. Statistical analysis was performed with a 2-tailed Student's *t* test for quantitative variables or with a chi-square test for qualitative variables. Quantitative data are expressed as the mean ± SD. $P < 0.05$ was considered to be statistically significant.

Acknowledgments

We thank Trevor Ralph for editorial assistance and Chikako Tanaka for helpful suggestions.

Received for publication August 13, 2007, and accepted in revised form November 7, 2007.

Address correspondence to: Naoki Tanaka, Department of Metabolic Regulation, Institute on Aging and Adaptation, Shinshu University Graduate School of Medicine, Asahi 3-1-1, Matsumoto 390-8621, Japan. Phone: 81-263-37-2850; Fax: 81-263-37-3094; E-mail: naopi@hsp.md.shinshu-u.ac.jp.

1. Kiyosawa, K., et al. 1990. Interrelationship of blood transfusion, non-A, non-B hepatitis and hepatocellular carcinoma: analysis by detection of antibody to hepatitis C virus. *Hepatology.* **12**:671–675.
2. Kiyosawa, K., et al. 2004. Hepatocellular carcinoma: recent trends in Japan. *Gastroenterology.* **127**(5 Suppl. 1):S17–S26.
3. Tanaka, Y., et al. 2002. Inaugural article: a comparison of the molecular clock of hepatitis C virus in the United States and Japan predicts that hepatocellular carcinoma incidence in the United States will increase over the next two decades. *Proc. Natl. Acad. Sci. U. S. A.* **99**:15584–15589.
4. Okuda, K., Fujimoto, I., Hanai, A., and Urano, Y. 1987. Changing incidence of hepatocellular carcinoma in Japan. *Cancer Res.* **47**:4967–4972.
5. El-Serag, H.B., and Mason, A.C. 1999. Rising incidence of hepatocellular carcinoma in the United States. *N. Engl. J. Med.* **340**:745–750.
6. Shimotohno, K. 2000. Hepatitis C virus and its pathogenesis. *Semin. Cancer Biol.* **10**:233–240.
7. Moriya, K., et al. 1997. Hepatitis C virus core protein induces hepatic steatosis in transgenic mice. *J. Gen. Virol.* **78**:1527–1531.
8. Shintani, Y., et al. 2004. Hepatitis C virus infection and diabetes: direct involvement of the virus in the development of insulin resistance. *Gastroenterology.* **126**:840–848.
9. Moriya, K., et al. 1998. The core protein of hepatitis C virus induces hepatocellular carcinoma in transgenic mice. *Nat. Med.* **4**:1065–1068.
10. Powell, E.E., Jonsson, J.R., and Clouston, A.D. 2005. Steatosis: co-factor in other liver diseases. *Hepatology.* **42**:5–13.
11. Ohata, K., et al. 2003. Hepatic steatosis is a risk factor for hepatocellular carcinoma in patients with chronic hepatitis C virus infection. *Cancer.* **97**:3036–3043.
12. Browning, J.D., and Horton, J.D. 2004. Molecular mediators of hepatic steatosis and liver injury. *J. Clin. Invest.* **114**:147–152.
13. Le, T.H., et al. 2004. The zonal distribution of megamitochondria with crystalline inclusions in nonalcoholic steatohepatitis. *Hepatology.* **39**:1423–1429.
14. Yang, S., Lin, H.Z., Hwang, J., Chacko, V.P., and Diehl, A.M. 2001. Hepatic hyperplasia in noncirrhotic fatty livers: is obesity-related hepatic steatosis a premalignant condition? *Cancer Res.* **61**:5016–5023.
15. Desvergne, B., and Wahli, W. 1999. Peroxisome proliferator-activated receptors: nuclear control of metabolism. *Endocr. Rev.* **20**:649–688.
16. Aoyama, T., et al. 1998. Altered constitutive expression of fatty acid-metabolizing enzymes in mice lacking the peroxisome proliferator-activated receptor α (PPARα). *J. Biol. Chem.* **273**:5678–5684.
17. Staels, B., et al. 1998. Mechanism of action of fibrates on lipid and lipoprotein metabolism. *Circulation.* **98**:2088–2093.
18. Harano, Y., et al. 2006. Fenofibrate, a peroxisome proliferator-activated receptor α agonist, reduces hepatic steatosis and lipid peroxidation in fatty liver Shionogi mice with hereditary fatty liver. *Liver Int.* **26**:613–620.
19. Yeldandi, A.V., Rao, M.S., and Reddy, J.K. 2000. Hydrogen peroxide generation in peroxisome proliferator-induced oncogenesis. *Mutat. Res.* **448**:159–177.
20. Yu, S., Rao, M.S., and Reddy, J.K. 2003. Peroxisome proliferator-activated receptors, fatty acid oxidation, steatohepatitis and hepatocarcinogenesis. *Curr. Mol. Med.* **3**:561–572.
21. Peters, J.M., Cattley, R.C., and Gonzalez, F.J. 1997. Role of PPARα in the mechanism of action of the nongenotoxic carcinogen and peroxisome proliferator Wy-14,643. *Carcinogenesis.* **18**:2029–2033.
22. Fan, C.Y., et al. 1998. Steatohepatitis, spontaneous peroxisome proliferation and liver tumors in mice lacking peroxisomal fatty acyl-CoA oxidase. Implications for peroxisome proliferator-activated receptor α natural ligand metabolism. *J. Biol. Chem.* **273**:15639–15645.
23. Moriya, K., et al. 2001. Oxidative stress in the absence of inflammation in a mouse model for hepatitis C virus-associated hepatocarcinogenesis. *Cancer Res.* **61**:4365–4370.
24. Lee, S.S., et al. 1995. Targeted disruption of the α isoform of the peroxisome proliferator-activated receptor gene in mice results in abolishment of the pleiotropic effects of peroxisome proliferators. *Mol. Cell. Biol.* **15**:3012–3022.
25. Mandard, S., Muller, M., and Kersten, S. 2004. Peroxisome proliferator-activated receptor α target genes. *Cell. Mol. Life Sci.* **61**:393–416.
26. Peters, J.M., et al. 1998. Role of peroxisome proliferator-activated receptor α in altered cell cycle regulation in mouse liver. *Carcinogenesis.* **19**:1989–1994.
27. Tsutsumi, T., et al. 2002. Interaction of hepatitis C virus core protein with retinoid X receptor α modulates its transcriptional activity. *Hepatology.* **35**:937–946.
28. Tanaka, N., et al. 2003. In vivo stabilization of nuclear retinoid X receptor α in the presence of peroxisome proliferator-activated receptor α. *FEBS Lett.* **543**:120–124.
29. Moriishi, K., et al. 2007. Critical role of PA28γ in hepatitis C virus-associated steatogenesis and hepatocarcinogenesis. *Proc. Natl. Acad. Sci. U. S. A.* **104**:1661–1666.
30. Perlemuter, G., et al. 2002. Hepatitis C virus core

protein inhibits microsomal triglyceride transfer protein activity and very low density lipoprotein secretion: a model of viral-related steatosis. *FASEB J.* **16**:185–194.
31. Korenaga, M., et al. 2005. Hepatitis C virus core protein inhibits mitochondrial electron transport and increases reactive oxygen species (ROS) production. *J. Biol. Chem.* **280**:37481–37488.
32. Gomez-Gonzalo, M., et al. 2004. Hepatitis C virus core protein regulates p300/CBP co-activation function. Possible role in the regulation of NF-AT1 transcriptional activity. *Virology.* **328**:120–130.
33. Yu, S., and Reddy, J.K. 2007. Transcription coactivators for peroxisome proliferator-activated receptors. *Biochim. Biophys. Acta.* **1771**:936–951.
34. Spaziani, A., Alisi, A., Sanna, D., and Balsano, C. 2006. Role of p38 MAPK and RNA-dependent protein kinase (PKR) in hepatitis C virus core-dependent nuclear delocalization of cyclin B1. *J. Biol. Chem.* **281**:10983–10989.
35. Diradourian, C., Girard, J., and Pegorier, J.P. 2005. Phosphorylation of PPARs: from molecular characterization to physiological relevance. *Biochimie.* **87**:33–38.
36. Reddy, J.K., Rao, M.S., Azarnoff, D.L., and Sell, S. 1979. Mitogenic and carcinogenic effects of a hypolipidemic peroxisome proliferator, [4-chloro-6-(2,3-xylidino)-2- pyrimidinylthio]acetic acid (Wy-14,643), in rat and mouse liver. *Cancer Res.* **39**:152–161.
37. Rao, M.S., and Reddy, J.K. 1996. Hepatocarcinogenesis of peroxisome proliferators. *Ann. N. Y. Acad. Sci.* **804**:573–587.
38. Genini, D., and Catapano, C.V. 2006. Control of peroxisome proliferator-activated receptor fate by the ubiquitin-proteasome system. *J. Recept. Signal. Transduct. Res.* **26**:679–692.
39. Dharancy, S., et al. 2005. Impaired expression of the peroxisome proliferator-activated receptor alpha during hepatitis C virus infection. *Gastroenterology.* **128**:334–342.
40. de Gottardi, A., et al. 2006. Peroxisome proliferator-activated receptor-alpha and -gamma mRNA levels are reduced in chronic hepatitis C with steatosis and genotype 3 infection. *Aliment. Pharmacol. Ther.* **23**:107–114.
41. Lefkowitch, J.H., et al. 1993. Pathological diagnosis of chronic hepatitis C: a multicenter comparative study with chronic hepatitis B. *Gastroenterology.* **104**:595–603.
42. Moriya, K., et al. 2001. Increase in the concentration of carbon 18 monounsaturated fatty acids in the liver with hepatitis C: analysis in transgenic mice and humans. *Biochem. Biophys. Res. Commun.* **281**:1207–1212.
43. Barbaro, G., et al. 1999. Hepatocellular mitochondrial alterations in patients with chronic hepatitis C: ultrastructural and biochemical findings. *Am. J. Gastroenterol.* **94**:2198–2205.
44. Hui, J.M., et al. 2003. Insulin resistance is associated with chronic hepatitis C virus infection and fibrosis progression [corrected]. *Gastroenterology.* **125**:1695–1704.
45. Kato, J., et al. 2001. Normalization of elevated hepatic 8-hydroxy-2'-deoxyguanosine levels in chronic hepatitis C patients by phlebotomy and low iron diet. *Cancer Res.* **61**:8697–8702.
46. Horiike, S., et al. 2005. Accumulation of 8-nitroguanine in the liver of patients with chronic hepatitis C. *J. Hepatol.* **43**:403–410.
47. Takenaka, K., et al. 1994. Possible multicentric occurrence of hepatocellular carcinoma: a clinicopathological study. *Hepatology.* **19**:889–894.
48. Oikawa, T., et al. 2005. Multistep and multicentric development of hepatocellular carcinoma: histological analysis of 980 resected nodules. *J. Hepatol.* **42**:225–229.
49. Akiyama, T.E., et al. 2001. Peroxisome proliferator-activated receptor-α regulates lipid homeostasis, but is not associated with obesity. *J. Biol. Chem.* **276**:39088–39093.
50. Nakajima, T., et al. 2004. Peroxisome proliferator-activated receptor α protects against alcohol-induced liver damage. *Hepatology.* **40**:972–980.
51. Ni, R., et al. 1994. Fas-mediated apoptosis in primary cultured mouse hepatocytes. *Exp. Cell Res.* **215**:332–337.
52. Graulet, B., Gruffat, D., Durand, D., and Bauchart, D. 1998. Fatty acid metabolism and very low density lipoprotein secretion in liver slices from rats and preruminant calves. *J. Biochem.* **124**:1212–1219.
53. Folch, J., Lees, M., and Sloane Stanley, G.H. 1957. A simple method for the isolation and purification of total lipids from animal tissues. *J. Biol. Chem.* **226**:497–509.
54. Gurtu, V., Kain, S.R., and Zhang, G. 1997. Fluorometric and colorimetric detection of caspase activity associated with apoptosis. *Anal. Biochem.* **251**:98–102.

Hepatology Research 2007; 37: S319–S326 doi: 10.1111/j.1872-034X.2007.00236.x

Innate immunity in hepatitis C virus infection: Interplay among dendritic cells, natural killer cells and natural killer T cells

Tatsuya Kanto[1,2] and Norio Hayashi[1]

[1]*Department of Gastroenterology and Hepatology and* [2]*Department of Dendritic Cell Biology and Clinical Applications, Osaka University Graduate School of Medicine, Osaka, Japan*

Sequential activation of innate and adaptive immune response is crucial for virus elimination. We thus sought to clarify the role of innate immune system in the pathogenesis of hepatitis C virus (HCV) infection. Dendritic cells (DC) sense virus infection via toll-like receptors (TLR) or retinoic acid inducible gene-I (RIG-I), resulting in the secretion of type-I interferons (IFN) and inflammatory cytokines. Blood DC consist of two subsets; myeloid DC (MDC) and plasmacytoid DC (PDC). In MDC from HCV-infected patients, regardless of higher expression of TLR2, TLR4 and RIG-I compared to the controls, the levels of TLR/RIG-I-mediated IFN-β or TNF-α induction are lower than those in uninfected donors. These results suggest that the signal transduction in the downstream of TLR/RIG-I in MDC is profoundly impaired in HCV infection. In response to IFN-α, DC are able to express MHC class-I related chain A/B (MICA/B) and activate natural killer (NK) cells following ligation of NKG2D. Interestingly, DC from HCV-infected patients are unresponsive to exogenous IFN-α to enhance MICA/B expression and fail to activate NK cells. Alternatively, NK cells from HCV-infected patients downregulate DC functions in the presence of human leukocyte antigen E-expressing hepatocytes by secreting interleukin (IL)-10 and transforming growth factor-β1. Such functional alteration of NK cells in HCV infection is ascribed to the enhanced expression of inhibitory receptor NKG2A/CD94 compared to the healthy counterparts. Invariant NKT cells activated by CD1d-positive DC secrete both T-helper (Th)1 and Th2 cytokines, serving as immune regulators. The frequency of NKT cells in chronic HCV infection does not differ from those in healthy donors. Activated NKT cells produce higher levels of IL-13 but comparable levels of IFN-γ with those from healthy subjects, showing that NKT cells are biased to Th2-type in chronic HCV infection. In conclusion, cross-talks among DC, NK cells and NKT cells are critical in shaping subsequent adaptive immune response against HCV.

Key words: α-galactosyl-ceramide, IL-β, MICA/B, NKG2A, TLR

INTRODUCTION

HEPATITIS C VIRUS (HCV) is one of major causes of chronic liver disease worldwide. HCV is hepatotrophic, but not directly cytopathic and elicits progressive liver injuries resulting in end-stage liver disease unless effectively eradicated.[1] Epidemiological studies have revealed that more than 80% of acutely HCV-infected patients fail to eradicate the virus and they subsequently develop chronic hepatitis.[1] It has been proposed that the ability of infected hosts to mount vigorous and sustained cellular immune reactions to HCV is necessary for control in primary infection.[2] Once HCV survives the initial interaction with the host immune system, it uses several means to nullify the selective immunological pressure during the later phases of infection. First, the virus alters its antigenic epitopes recognized by T cells and neutralizing antibodies to escape immune surveillance. Second, HCV also subverts immune functions in an antigen-specific manner, from innate to adaptive immunity.[3]

Cumulative reports have shown that innate immune system dictates the direction and magnitude of subsequent adaptive immune response. It is generally accepted that HCV-specific $CD8^+$ T cells are responsible for HCV elimination by inducing hepatocyte apoptosis.[2] Innate immune cells, including natural killer (NK) cells and

Correspondence: Tatsuya Kanto M.D., PhD, Department of Gastroenterology and Hepatology, Osaka University Graduate School of Medicine, 2-2 Yamada-oka, Suita, Osaka 565-0871, Japan. Email: kantot@gh.med.osaka-u.ac.jp

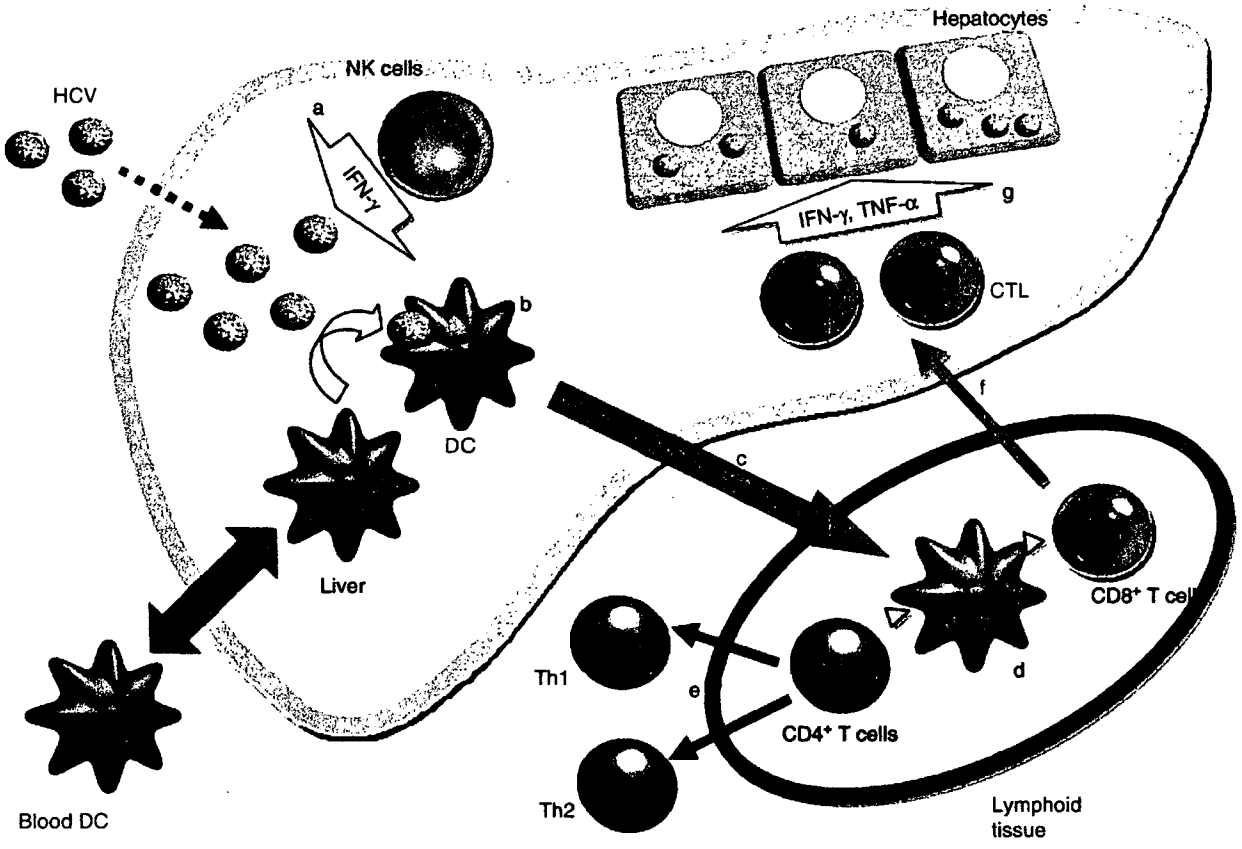

Figure 1 Key players in immune reactions in viral hepatitis. CTL, cytotoxic T lymphocyte; DC, dendritic cell; HCV, hepatitis C virus; NK, natural killer cell; Th, helper T cell. (1–7), see text.

NKT cells, may contribute to HCV eradication after primary infection; however, their roles in a chronically infected state remain elusive. Because dendritic cells (DC) orchestrate anti-HCV immune response by linking innate and adaptive arms of the immune system,[4] functional impairment of DC leads to failure of NK cells, NKT cells, $CD4^+$ and $CD8^+$ T cells. Infiltration of disabled $CD8^+$ T cells to the infected liver may result in weak liver inflammation that is not sufficient for HCV eradication.[5]

In this paper, we discuss the current understandings of the roles of innate immunity in the pathogenesis of HCV infection, especially focused on interferons (IFN), DC, NK cells and NKT cells.

KEY PLAYERS IN IMMUNE RESPONSES TO VIRAL HEPATITIS

AFTER HCV INFECTS the liver, viral replication continues and viral particles are continuously released into the circulation. The first lines of defense are provided by NK and NKT cells, of which populations are relatively increased in the liver compared to the periphery. These cells are activated in the liver, where expression of IFN-α and IFN-inducible genes are extremely high during the early phase of hepatitis virus infection.[6] Activated NK and NKT cells secrete IFN-γ, which inhibits replication of HCV through a non-cytolytic mechanism (Fig. 1a).[7]

Dendritic cells or resident macrophages in the liver are capable of taking up viral antigens, and processing and presenting them to other immune cells (Fig. 1b).[4] Because DC express distinct sets of toll-like receptors (TLR),[8] it is likely that some viral components stimulate DC through cytosolic ligation of TLR. DC develop a mature phenotype and migrate to lymphoid tissues (Fig. 1c), where they stimulate effectors, including T cells and B cells (Fig. 1d). Following the encounter of DC with other cells, DC secrete various cytokines (interleukin [IL]-12, tumor necrosis factor [TNF]-α, IFN-α and IL-10) instructing or regulating the functions of the adja-

cent cells.[4] In addition to these cytokines, DC express various costimulatory molecules and ligands to enhance or limit the functions of immune and infected cells. The existence of functionally and ontogenetically distinct DC subsets has been reported; that is, myeloid DC (MDC) and plasmacytoid DC (PDC).[9] MDC predominantly produce IL-12 or TNF-α following proinflammatory stimuli, while PDC release a considerable amount of IFN-α upon virus infection depending on the immune stimulus; both cytokines in actuality can be made by both cells. Helper T cells have an immunoregulatory function mediated by the secretion of cytokines that support either cytotoxic T lymphocyte (CTL) generation (T-helper [Th]1 with secretion of IL-2, IFN-γ and TNF-α) or B-cell function and antibody production (Th2 with secretion of IL-4, IL-5, IL-10 and IL-13) (Fig. 1e). DC ontogeny and DC-derived cytokines are crucially associated with the polarization of helper T-cell subsets.

It is generally accepted that adaptive immunity performs a critical role during the clinical courses of hepatitis. The involvement of antigen-specific $CD4^+$ T cells in HCV eradication has been well described during both acute or chronic infection.[10] However, there is little evidence that $CD4^+$ T cells mediate direct liver cell injury in HCV infection. Thus, it is likely that $CD4^+$ T cells play a critical role in facilitating other antiviral immune mechanisms, such as enhancing $CD8^+$ effector function. The antigen-primed CTL recruit to the liver (Fig. 1f) and constitute the critical element in the eradication of virus-infected cells (Fig. 1g).

INNATE IMMUNITY IN HCV INFECTION

Toll-like receptors and retinoic acid inducible gene-I as sensors for virus infection

GENE EXPRESSION ANALYSES in HCV-infected liver revealed that HCV triggers expression of type I IFN and IFN-induced genes during primary infection regardless of the outcomes.[6] However, the HCV viral load does not decrease in the early phase, suggesting that HCV impedes the execution of antiviral machineries. Several HCV-derived proteins are involved in the suppression on the signaling pathways inducing antiviral proteins, such as interferon regulatory factor (IRF)-3,[11] nuclear factor (NF)-κB and double-stranded RNA-dependent protein kinases (PKR).[12] Mammalian TLR sense some pathogen-associated molecular patterns embedded in virus components and then induce inflammatory cytokines or type-I IFN, resulting in the augmentation of antivirus immune reactions.[8] Retinoic acid inducible gene-I (RIG-I) is a cytosolic molecule that senses double-stranded RNA (dsRNA) of virus replicative intermediate, which subsequently activates IRF-3 and NF-κB pathways.[13] By using the HCV subgenomic replicon system, it has been demonstrated that HCV NS3/4 A proteins influence the functions of adaptor molecules mediating TLR-dependent and RIG-I-dependent pathways, resulting in an impairment of the induction of IFN-β as well as subsequent IFN-stimulated genes.[14,15] However, it is yet to be proven whether the results obtained from HCV replicon are applicable or not for HCV-infected individuals.

To investigate the roles of TLR/RIG-I in HCV infection, we compared their expressions and functions in MDC and PDC between patients and donors. In MDC from HCV-infected patients, TLR2, TLR4 and RIG-I expression were significantly higher than those in healthy counterparts. Of particular interest, regardless of the higher expressions, specific agonists for these sensors stimulated patients' MDC to induce lesser amounts of IFN-β and TNF-α compared to donor MDC (Miyazaki *et al.*, 2007, unpublished data). These results show that the signal transduction via these receptors is strongly impeded in HCV infection. Inconsistent with the findings of MDC, we previously reported that TLR2 expression on monocyte-derived DC (MoDC) in chronic hepatitis C is lower than those in healthy donors.[16] Because MoDC is an *in vitro*-generated DC mimic, the opposite results of TLR2 in HCV infection might be explained by impaired ability of MoDC to mature in response to cytokines, as reported elsewhere.[17] Further investigation is needed to clarify which TLR or RIG-I is predominantly utilized by HCV to evoke immune reactions.

Blood DC subsets

Impaired antigen presentation by DC might be involved in the failure of the maintenance of sustained HCV-specific T-cell response. MoDC generated from hepatitis C patients have an impaired ability to stimulate allogeneic $CD4^+$ T cells.[18,19] Functional impairment of DC diminished when HCV had been eradicated from patients, revealing the evidence of HCV-induced DC disability.[18] In addition to *in vitro*-generated DC, the alterations in number and function of circulating blood DC have been reported in HCV infection.[20]

Direct HCV infection of DC might be one of the plausible mechanisms of DC dysfunction in chronic hepatitis C. The HCV genome has been reported to be isolated